

Budget of nitrous acid (HONO) and its impacts on atmospheric oxidation capacity at an urban site in the fall season of Guangzhou, China

Yihang Yu^{1,2,†}, Peng Cheng^{1,2,5,*,†}, Huirong Li^{1,2}, Wenda Yang^{1,2}, Baobin Han^{1,2}, Wei Song³, Weiwei Hu³, Xinming Wang³, Bin Yuan^{4,5}, Min Shao^{4,5}, Zhijiong Huang⁴, Zhen Li⁴, Junyu Zheng^{4,5}, Haichao Wang⁶ and Xiaofang Yu^{1,2}

¹Institute of Mass Spectrometry and Atmospheric Environment, Jinan University, Guangzhou 510632, China

²Guangdong Provincial Engineering Research Center for Online Source Apportionment System of Air Pollution, Guangzhou 510632, China

10 ³State Key Laboratory of Organic Geochemistry, Guangzhou Institute of Geochemistry, Chinese Academy of Sciences, Guangzhou 510640, China

⁴Institute for Environmental and Climate Research, Jinan University, Guangzhou 511443, China

⁵Guangdong-Hongkong-Macau Joint Laboratory of Collaborative Innovation for Environmental Quality, Guangzhou 511443, China

15 ⁶School of Atmospheric Sciences, Sun Yat-Sen University, Zhuhai, China.

†These authors contribute equally to this paper.

*Correspondence to: Peng Cheng (chengp@jnu.edu.cn)

Abstract. Nitrous acid (HONO) can produce hydroxyl radicals (OH) by photolysis and plays an important role in atmospheric photochemistry. Over the years, high concentrations of HONO have been observed in the Pearl River Delta region (PRD) of China, which may be one reason for the elevated atmospheric oxidation capacity. A comprehensive atmospheric observation campaign was conducted at an urban site in Guangzhou from 27 September to 9 November 2018. During the period, HONO was measured from 0.02 to 4.43 ppbv with an average of 0.74 ± 0.70 ppbv. The emission ratios (HONO/NO_x) of $0.9 \pm 0.4\%$ were derived from 11 fresh plumes. The primary emission rates of HONO at night were calculated to be between 0.04 ± 0.02 ppbv h⁻¹ and 0.30 ± 0.15 ppbv h⁻¹ based on a high-resolution emission inventory. The HONO formation rate by the homogeneous reaction of OH + NO at night was 0.26 ± 0.08 ppbv h⁻¹, which can be seen as secondary results from primary emission. They were both much higher than the increase rate of HONO (0.02 ppbv h⁻¹) during night. The soil emission rate of HONO at night was calculated to be 0.019 ± 0.001 ppbv h⁻¹. Assuming dry deposition as the dominant removal process of HONO at night, a deposition velocity of at least ~ 1.8 cm s⁻¹ is required to balance the direct emissions and OH + NO reaction. Correlation analysis shows that NH₃ and relative humidity (RH) may participate in the heterogeneous transformation from NO₂ to HONO at night. In the daytime, the average primary emission P_{emis} was 0.12 ± 0.01 ppbv h⁻¹, and the homogeneous reaction $P_{\text{OH+NO}}$ was 0.79 ± 0.61 ppbv h⁻¹, larger than the unknown sources P_{Unknown} (0.65 ± 0.46 ppbv h⁻¹). These results suggest primary emissions as a key factor affecting HONO at our site, both during daytime and nighttime. Similar to previous studies, the daytime unknown source of HONO, P_{Unknown} , appeared to be related

to the photo-enhanced conversion of NO₂. The daytime average OH production rates by photolysis of HONO was 3.7×10^6 cm⁻³ s⁻¹, lower than that from O¹D + H₂O at 4.9×10^6 cm⁻³ s⁻¹. Simulations of OH and O₃ with the Master Chemical Mechanism (MCM) box model suggested strong enhancement effect of HONO on OH and O₃ by 59% and 68.8%, respectively, showing a remarkable contribution of HONO to the atmospheric oxidation in the fall season of Guangzhou.

Keywords: HONO; Atmospheric oxidation capacity; Budget analysis; Heterogeneous reaction

40 1 Introduction

As a primary source of hydroxyl radical (OH), HONO has attracted scientific researchers' great interest. The photolysis of HONO (Reaction R1) can generate a substantial amount of OH, which is a primary atmosphere oxidant that is responsible for oxidizing and removing of most natural and anthropogenic trace gases. Additionally, OH radicals can initiate the oxidation of the volatile organic compounds (VOC) to produce hydroperoxyl radicals (HO₂) and organic peroxy radicals (RO₂). These free radicals can further lead to the formation of ozone (O₃) in the presence of nitrogen oxides (NO_x) (Xue et al., 2016; Finlayson-Pitts and Pitts, 2000; Hofzumahaus et al., 2009; Lelieveld et al., 2016; Tan et al., 2018). Up to 33–92% OH formation can be attributed to HONO photolysis in both rural and urban sites (Kleffmann et al., 2005; Michoud et al., 2012; Tan et al., 2017; Xue et al., 2020; Hendrick et al., 2014). However, the detailed formation mechanisms of HONO are still not well understood and the observed HONO concentrations cannot be completely explained by current research (Sörgel et al., 2011a; Kleffmann et al., 2005; Sarwar et al., 2008; Liu et al., 2019a; Lee et al., 2016; Liu et al., 2020c).



HONO sources generally include direct emissions, homogeneous reactions and heterogeneous reactions. HONO can be directly emitted into the troposphere from combustion processes such as biomass burning, vehicle exhaust, domestic heating, and industrial exhaust (Liu et al., 2019b; Neuman et al., 2016; Nie et al., 2015; Kramer et al., 2020). The emission ratios of HONO/NO_x of traffic sources have been estimated in the range of 0.3%–0.85% through tunnel experiments considering various engine types (Kirchstetter et al., 1996; Kurtenbach et al., 2001; Kramer et al., 2020). Soil nitrite formed through the processes of biological nitrification and denitrification, were proposed to be a prominent HONO source in the troposphere (Maljanen et al., 2013; Oswald et al., 2013; Wu et al., 2019; Su et al., 2011). Subsequently, biological soil crusts (biocrusts) were also found to release HONO (Weber et al., 2015; Porada et al., 2019; Meusel et al., 2018). In addition, an acid displacement mechanism has also been suggested to contribute substantial fraction of daytime HONO formation (VandenBoer et al., 2015). The reaction between NO and OH is considered an important pathway of HONO formation when OH and NO concentrations are relatively high (Alicke et al., 2002; Li et al., 2012; Pagsberg et al., 1997; Qin et al., 2009; Wong et al., 2011), whereas this pathway often cannot explain the observed HONO concentrations, especially during

daytime (Tang et al., 2015; Li et al., 2010; Czader et al., 2012; Tong et al., 2016). Bejan et al. (2006) studied the HONO formation by the photolysis of different gaseous nitrophenols and proposed that the photolysis of nitrophenols can partly explain the observed HONO formation in the urban atmosphere. Zhang and Tao (2010) proposed that HONO can form through homogeneous nucleation of NH_3 , NO_2 and H_2O . However, this reaction has not yet been observed in field experiments nor tested by laboratory studies. Li et al. (2014b) proposed that the reaction of NO_2 with $\text{HO}_2\text{-H}_2\text{O}$ could be a gas-phase source of HONO in the lower troposphere. But Ye et al. (2015) estimated the HONO yield of the reaction of NO_2 with $\text{HO}_2\text{-H}_2\text{O}$ was only 3%. Additionally, heterogeneous reactions on different kinds of surfaces have also been found to be possible significant HONO sources, including heterogeneous reactions of NO_2 on ground surfaces (Meusel et al., 2016; VandenBoer et al., 2013), building surfaces (Acker et al., 2006; Indarto, 2012), ocean surfaces (Wen et al., 2019; Wojtal et al., 2011; Yang et al., 2021a), soil surfaces (Laufs et al., 2017; Kleffmann et al., 2003; Yang et al., 2021b) and vegetation surfaces (Stutz et al., 2002; Marion et al., 2021), etc. Photosensitized reduction reaction of NO_2 on organic surfaces (such as humic acids and aromatics) has been considered as an effective pathway to generate HONO (George et al., 2005; Stemmler et al., 2006; Liu et al., 2020a; Ammar et al., 2010; Brigante et al., 2008; Cazoir et al., 2014; Sosedova et al., 2011). The heterogeneous conversion of NO_2 to HONO on humid surfaces have also been studied (Finlayson-Pitts et al., 2003; Ammann et al., 1998; Ndour et al., 2008) and this conversion can be further promoted by ambient NH_3 and SO_2 (Ge et al., 2019; Wang et al., 2016; Xu et al., 2019; Li et al., 2018b; Wang et al., 2021). In addition, HONO can also be formed by heterogeneous conversion of NO_2 on secondary organic aerosols and fresh soot particles (Arens et al., 2001; Ziemba et al., 2010), but the contributions and mechanisms are still under discussion (Arens et al., 2001; Aubin and Abbatt, 2007; Bröske et al., 2003; Qin et al., 2009). Both field observations and laboratory studies found that the photolysis of adsorbed HNO_3 and particulate nitrate (NO_3^-) made an important contribution to HONO formation (Ye et al., 2016; Ye et al., 2017; Zhou et al., 2003; Zhou et al., 2002b; Zhou et al., 2011; Ziemba et al., 2010). However, Laufs and Kleffmann (2016) obtained a very low HNO_3 photolysis frequency in laboratory, almost two orders of magnitude lower than the result by Zhou et al. (2003).

The Pearl River Delta (PRD) region is one of the biggest city clusters in the world with dense population and large anthropogenic emissions. Rapid economic development and urbanization have led to severe deterioration of air quality in this region, which was characterized by atmospheric "compound pollution" with concurrent high fine particulate matter ($\text{PM}_{2.5}$) and ozone (O_3) (Tang, 2004; Chan and Yao, 2008; Yue et al., 2010; Wang et al., 2017b; Xue et al., 2014; Zheng et al., 2010). While O_3 has been increasing along with reduced $\text{PM}_{2.5}$ over recent years in the region (Li et al., 2014a; Liao et al., 2020; Wang et al., 2009; Zhong et al., 2013; Lu et al., 2018), and has become the dominant factor of the air quality index exceeding the national standard (Feng et al., 2019), indicating the enhancement of atmospheric oxidation capacity. By far two comprehensive atmospheric observations were conducted in the PRD region to detect OH radicals. High concentrations of OH radicals were observed both times, especially in the first time it was the highest ever-reported, which cannot be explained by the current knowledge of atmospheric chemistry (Hofzumahaus et al., 2009). Substantial level of HONO was suggested to be the major source of the OH- HO_2 - RO_2 radical system in above two campaigns (Lu et al., 2012; Tan et al.,

100 2019a). Moreover, high concentrations of HONO have also been confirmed in other observations in this area during last two decades (Hu et al., 2002; Su et al., 2008b; Su et al., 2008a; Qin et al., 2009; Li et al., 2012; Shao et al., 2004). Fast OH production through HONO photolysis may be a key factor for the increasing atmospheric oxidation capacity and ozone concentration in this area.

105 In this work, we performed continuous measurements of HONO, along with trace gases, photolysis frequencies and meteorological conditions at an urban site in Guangzhou from 27 September to 9 November 2018, as part of the field campaign named "Particles, Radicals, Intermediates from oxidation of primary Emissions in Greater Bay Area" (PRIDE-GBA2018). Benefiting from numerous prior field observational studies in the PRD region, our study stands in a strong position to ensure high quality of data acquisition and analysis of HONO, along with a full suite of other chemical species,
110 providing a unique and valuable opportunity to refine our knowledge of HONO sources and sinks, as well as the role of HONO in the photochemistry of O₃ and OH in such a region with extensive air pollution as well as rigorous emission control over recent years. A high resolution (3 km × 3 km) NO_x emission inventory for the Guangzhou city (Huang et al., 2021) was used to estimate the primary emission rates of NO_x and HONO, which would reduce the uncertainty of HONO primary emission rate. By analysing our observational data, both nighttime HONO formation pathways and daytime HONO budgets
115 have been investigated in this study. The contribution of HONO photolysis to OH production has been calculated and compared with that of O₃ photolysis and ozonolysis of alkenes. The impact of HONO on atmospheric oxidation capacity and O₃ formation is further investigated using a chemical box model based on Master Chemical Mechanism (MCMv3.3.1).

2 Experiment

120 2.1 Observation site

The sampling site (23.14° N, 113.36° E) is located in the Guangzhou Institute of Geochemistry Chinese Academy of Sciences (GIGCAS). The instruments were deployed in the cabin on the rooftop of a seven-story building (~ 40 m above the ground). The site is surrounded by residential communities and schools, with no industrial manufacturers or power plants around, representing a typical urban environment in the PRD region. The south China Expressway and Guangyuan
125 Expressway, both with heavy traffic loading, are located at west and south of the site, with distances of about 300 m. As a result, the site often experienced local emissions from traffic. The location and surroundings of the site are shown in Fig. S1.

2.2 Measurements

HONO was measured by a custom-built LOPAP (LOng Path Absorption Photometer) (Heland et al., 2001; Kleffmann et al., 2006). More information about our custom-built LOPAP (including principle, quality assurance/quality control, instrument
130 parameters and intercomparison) are introduced in supplement information.

In addition to HONO, ambient VOCs were measured using a TH-300B On-Line VOCs Monitoring System involving detection technology of ultralow temperature preconcentration coupled with gas chromatography-mass spectrometry (GC/MS) with the time resolution of 1 h. NO_x (NO + NO₂) was measured by a nitrogen oxides analyzer (Thermo Scientific, Model 42i), which used a NO-NO_x chemiluminescence detector equipped with a molybdenum-based converter with the time resolution and detection limit of 1 min and 1 ppbv respectively. It should be noted that the molybdenum oxide (MoO) converters may also convert some NO_z (= NO_y - NO_x) (e.g., HONO, peroxyacetyl nitrate (PAN), HNO₃, and so on.) species to NO and hence could overestimate the ambient NO₂ concentrations. The degree of overestimation depends on both air mass age and the composition of NO_y. At our site that was greatly affected by fresh emissions, the relative interferences of NO_z to NO₂ have been estimated to be around 10%, which is closed to the results of Xu et al. (2013) and negligible for our discussion of HONO budget. O₃ was measured by an O₃ analyzer (Thermo Scientific, Model 49i) via ultraviolet absorption method with the time resolution and detection limit of 1 min and 1 ppbv respectively. SO₂ was measured by SO₂ analyzer (Thermo Scientific, Model 43i) via pulsed fluorescence method with the time resolution and detection limit of 1 min and 1 ppbv respectively. CO was measured by a CO analyzer (Thermo Scientific, Model 48i) with the time resolution and detection limit of 1 min and 0.1 ppmv respectively. NH₃ was measured by laser absorption spectroscopy (PICARRO, G2508) with the time resolution and detection limit of 1 min and 1 ppbv respectively. Gaseous HNO₃ was detected by a Time-Of-Flight Chemical Ionization Mass Spectrometer (Aerodyne Research Inc., TOF-CIMS) with a time resolution of 1 min. And particulate nitrate (NO₃⁻) was measured by Time-Of-Flight Accelerator Mass Spectrometry (Aerodyne Research Inc., TOF-AMS) with a time resolution of 1 min. PM_{2.5} was measured by a Beta Attenuation Monitor (MET One Instruments Inc., BAM-1020) with the time resolution and detection limit of 1 h and 4.0 μg m⁻³ respectively. The meteorological data, including temperature (T), relative humidity (RH) and wind speed and direction (WS, WD) were recorded by Vantage Pro2 Weather Station (Davis Instruments Inc., Vantage Pro2) with the time resolution of 1 min. Photolysis frequencies including J(HONO), J(NO₂), J(H₂O₂) and J(O¹D) were measured by a filter radiometry (Focused Photonics Inc., PFS-100) with a time resolution of 1 min.

155 2.3 Box model

To evaluate the influence of HONO chemistry on the atmospheric oxidation capacity, a zero dimensional box model (Framework for 0-Dimensional Atmospheric Modeling–FOAM) based on the Master Chemical Mechanism (MCMv3.3.1) (Wolfe et al., 2016; Jenkin et al., 2003; Jenkin et al., 2015) was applied to calculate the concentrations of O₃ and OH radicals. The Master Chemical Mechanism describes atmospheric gas-phase organic chemistry in detail which has been widely used in atmospheric chemistry modelling. Kinetic rate coefficients were derived from the MCM v3.3.1 website (<http://mcm.leeds.ac.uk/MCM>). The model was implemented in MATLAB 2012. In this work, the boundary layer diurnal cycle has been modified and the dilution factor k_{dil} was set at 86400⁻¹ s. The solar zenith angle was calculated based on

longitude, latitude and time of the observation. Photolysis rate correction coefficient j_{corr} was set to 1. The model simulation was constrained by hourly averaged measurement data, including HONO, NO, NO₂, CO, SO₂, VOC species (listed in Table S2), and temperature, water vapor, wind speed, wind direction, pressure and photolysis frequencies $J(\text{NO}_2)$, $J(\text{HONO})$, $J(\text{O}^1\text{D})$ and $J(\text{H}_2\text{O}_2)$. Other non-measured photolysis frequencies were calculated according to Eq. (1) (Jenkin et al., 1997), and then scaled by the measured $J(\text{NO}_2)$:

$$J_i = L_i \cos(\chi)^{M_i} \exp(-N_i \sec(\chi)) \quad (1)$$

where χ represents the solar zenith angle (SZA); L_i , M_i and N_i are the photolysis parameters under clear sky conditions which were taken from Jenkin et al. (1997). The heterogeneous processes as well as deposition of chemical species were not considered in this model. The simulation results were evaluated by comparing against the measurements, and index of agreement (IOA), a statistical parameter was employed for the evaluation (Jeon et al., 2018; Xing et al., 2019; Li et al., 2010). Two simulations with and without HONO constrained by measured values were conducted to examine the impact of HONO on OH and O₃ formation.

175 3 Results and discussion

3.1 Data overview

The time series of meteorological parameters and pollutants during the campaign are shown in Fig. 1. The HONO concentrations ranged from 0.02 to 4.43 ppbv with an average of 0.74 ± 0.70 ppbv. Table 1 summarizes the HONO observations reported in PRD region since 2002. HONO appears to have shown a decreasing trend in Guangzhou, as improvement of air quality in Guangzhou was witnessed during the past decade. Spikes of NO occurred frequently, even up to 134.8 ppbv, as a result of traffic emissions from two major roads near the site. The concentrations of NO₂, SO₂, NH₃ and PM_{2.5} ranged from 5.4–102.0 ppbv, 0–6.3 ppbv, 2.8–7.8 ppbv and 4–109 $\mu\text{g m}^{-3}$ respectively with the average values of 50.8 ± 17.2 ppbv, 1.9 ± 1.2 ppbv, 6.3 ± 2.7 ppbv, and $36 \pm 16 \mu\text{g m}^{-3}$ respectively. The O₃ concentrations ranged from 0.3–149.8 ppbv with an average peak concentration of 73.9 ± 28.4 ppbv. During the observation, the temperature ranged from 17 °C to 30 °C with an average of 24 ± 3 °C, and the relative humidity ranged from 28% to 97% with an average of $70 \pm 17\%$. The average wind speed was $6.8 \pm 4.5 \text{ m s}^{-1}$, while the maximum wind speed was 22.7 m s^{-1} . There was a pollution period from 8th to 10th October with elevated PM_{2.5} ($60 \pm 12 \mu\text{g m}^{-3}$) and HONO (0.94 ± 0.58 ppbv). By contrast, from 29 October to 3 November, efficient ventilation driven by strong winds ($> 11 \text{ m s}^{-1}$) led to low levels of most pollutants in this period, with average concentrations of PM_{2.5} and HONO at $28 \pm 11 \mu\text{g m}^{-3}$ and 0.56 ± 0.34 ppbv, respectively.

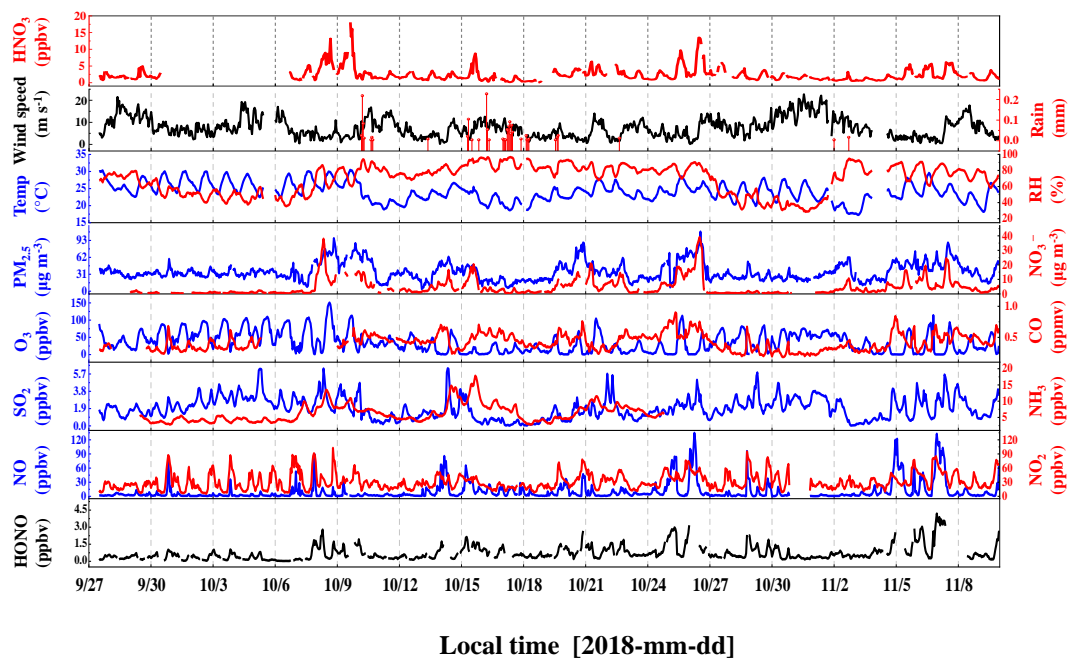


Figure 1. Temporal variations of meteorological and pollutants during the observation period.

Table 1. Overview of the ambient HONO, NO₂ and NO_x measurement, as well as the ratios of HONO/NO₂ in the PRD region ordered chronologically. Data from Guangzhou are in italic.

195

Location	Date	HONO (ppbv)		NO ₂ (ppbv)		NO _x (ppbv)		HONO/NO ₂		Reference	
		Night	Day	Night	Day	Night	Day	Night	Day		
<i>Guangzhou</i>	<i>Jul 2002</i>	<i>1.89</i>	–	–	–	–	–	–	–	<i>1</i>	
<i>(China)</i>	<i>Nov 2002</i>	<i>1.52</i>	–	–	–	–	–	–	–		
<i>Xinken</i>	<i>Oct–Nov 2004</i>	<i>1.20</i>	<i>1.30</i>	<i>0.80</i>	<i>34.8</i>	<i>30.0</i>	<i>37.8</i>	<i>40.0</i>	<i>0.037</i>	<i>0.027</i>	<i>2</i>
<i>Back Garden</i>	<i>Jul 2006</i>	<i>0.93</i>	<i>0.95</i>	<i>0.24</i>	<i>16.5</i>	<i>4.5</i>	<i>20.9</i>	<i>5.5</i>	<i>0.057</i>	<i>0.053</i>	<i>3</i>
<i>Guangzhou</i>	<i>Jul 2006</i>	<i>2.80</i>	<i>3.50</i>	<i>2.00</i>	<i>20.0</i>	<i>30.0</i>	–	–	<i>0.175</i>	<i>0.067</i>	<i>4</i>
<i>Guangzhou</i>	<i>Oct 2015</i>	<i>1.64</i>	<i>2.25</i>	<i>0.90</i>	<i>40.5</i>	<i>27.3</i>	<i>57.9</i>	<i>39.8</i>	<i>0.060</i>	<i>0.030</i>	<i>5</i>
<i>Guangzhou</i>	<i>Jul 2016</i>	<i>1.03</i>	<i>1.27</i>	<i>0.70</i>	<i>35.0</i>	<i>25.9</i>	<i>66.3</i>	<i>52.1</i>	<i>0.040</i>	<i>0.070</i>	<i>6</i>
<i>This work</i>	<i>Sep–Nov 2018</i>	<i>0.74</i>	<i>0.91</i>	<i>0.44</i>	<i>36.9</i>	<i>23.3</i>	<i>47.7</i>	<i>30.1</i>	<i>0.026</i>	<i>0.022</i>	
<i>Jiangmen</i>	<i>Oct–Nov 2008</i>	<i>0.60</i>	–	<i>0.48</i>	–	–	–	<i>9.1</i>	–	–	<i>7</i>
	<i>Aug 2011</i>	<i>0.66</i>	<i>0.66</i>	<i>0.70</i>	<i>21.8</i>	<i>18.1</i>	<i>29.3</i>	<i>29.3</i>	<i>0.031</i>	<i>0.042</i>	
<i>Hong Kong</i>	<i>Nov 2011</i>	<i>0.93</i>	<i>0.95</i>	<i>0.89</i>	<i>27.2</i>	<i>29.0</i>	<i>37.2</i>	<i>40.6</i>	<i>0.034</i>	<i>0.030</i>	<i>8</i>
<i>(China)</i>	<i>Feb 2012</i>	<i>0.91</i>	<i>0.88</i>	<i>0.92</i>	<i>22.2</i>	<i>25.8</i>	<i>37.8</i>	<i>48.3</i>	<i>0.036</i>	<i>0.035</i>	
	<i>May 2012</i>	<i>0.35</i>	<i>0.33</i>	<i>0.40</i>	<i>14.7</i>	<i>15.0</i>	<i>19.1</i>	<i>21.1</i>	<i>0.022</i>	<i>0.030</i>	
<i>Hong Kong</i>	<i>Sep–Dec 2012</i>	<i>0.13</i>	–	–	–	–	–	–	–	–	<i>9</i>
<i>(China)</i>											
<i>Heshan</i>	<i>Oct 2013</i>	<i>1.57</i>	–	–	–	–	–	–	–	–	<i>10</i>
<i>(China)</i>											
<i>Heshan</i>	<i>Oct–Nov 2014</i>	<i>1.40</i>	<i>1.78</i>	<i>0.77</i>	<i>19.3</i>	<i>17.9</i>	<i>21.5</i>	<i>22.7</i>	<i>0.093</i>	<i>0.055</i>	<i>11</i>
<i>(China)</i>											
<i>Hong Kong</i>	<i>Mar–May 2015</i>	<i>3.30</i>	<i>2.86</i>	<i>3.91</i>	–	–	–	–	–	–	<i>12</i>
<i>(China)</i>											
<i>Heshan</i>	<i>Jan 2017</i>	<i>2.70</i>	<i>3.10</i>	<i>2.30</i>	–	–	–	–	<i>0.116</i>	<i>0.089</i>	<i>13</i>
<i>(China)</i>											

References: 1. Hu et al. (2002); 2. Su et al. (2008a) and (Su et al., 2008b); 3. Su (2008) and Li et al. (2012); 4. Qin et al. (2009); 5. Tian et al. (2018); 6. Yang et al. (2017a); 7. Yang (2014); 8. Xu et al. (2015); 9. Zha et al. (2014); 10. Yue et al. (2016); 11. Liu (2017); 12. Yun et al. (2017). 13. Yun (2018)

200

The time series of photolysis frequencies $J(\text{HONO})$, $J(\text{O}^1\text{D})$ and $J(\text{NO}_2)$ in the whole observation period are shown in Fig. S3. The maximum values of $J(\text{HONO})$, $J(\text{O}^1\text{D})$ and $J(\text{NO}_2)$ are $1.58 \times 10^{-3} \text{ s}^{-1}$, $2.54 \times 10^{-5} \text{ s}^{-1}$ and $9.31 \times 10^{-3} \text{ s}^{-1}$, respectively. These J values tracked a similar diurnal pattern, reaching a maximum at noon with high solar radiation and decreasing to zero at night.

205

The diurnal variations of HONO, NO_2 , HONO/ NO_2 , and NO are shown in Fig. 2. A daytime trough and a night-time peak of HONO were observed, as typically seen in cities and rural sites (Lee et al., 2016; Xue et al., 2020; Villena et al., 2011; Yang et al., 2021c). The observed high HONO concentration around 0.5 ppbv at daytime implies strong HONO production to balance its rapid loss through photolysis. NO_2 showed a similar diurnal pattern. It is worth noting that the diurnal variation of
210 NO was quite similar to that of HONO, implying the potential association between them. Additionally, the observed large amount of NO (10.8 ± 17.2 ppbv) at night indicates strong primary emission near the site. As an indicator of NO_2 to HONO conversion, the ratio of HONO/ NO_2 rose at night and decreased after sunrise due to photolysis, ranging from 0.2% to 9.1% with an average of $2.3 \pm 1.3\%$, which is lower than most previous field observations in PRD region (Li et al., 2012; Qin et al., 2009; Xu et al., 2015), and is typical for relatively fresh plumes. Previous many field observations also reported low values
215 of HONO/ NO_2 ranging from 2% to 10% in freshly polluted air masses (Febo et al., 1996; Lammel and Cape, 1996; Sörgel et al., 2011b; Stutz et al., 2004; Zhou et al., 2007; Su et al., 2008a). The relatively stable and low value of HONO/ NO_2 in nighttime seems to indicate the low contribution of heterogeneous reactions of NO_2 to HONO concentrations.

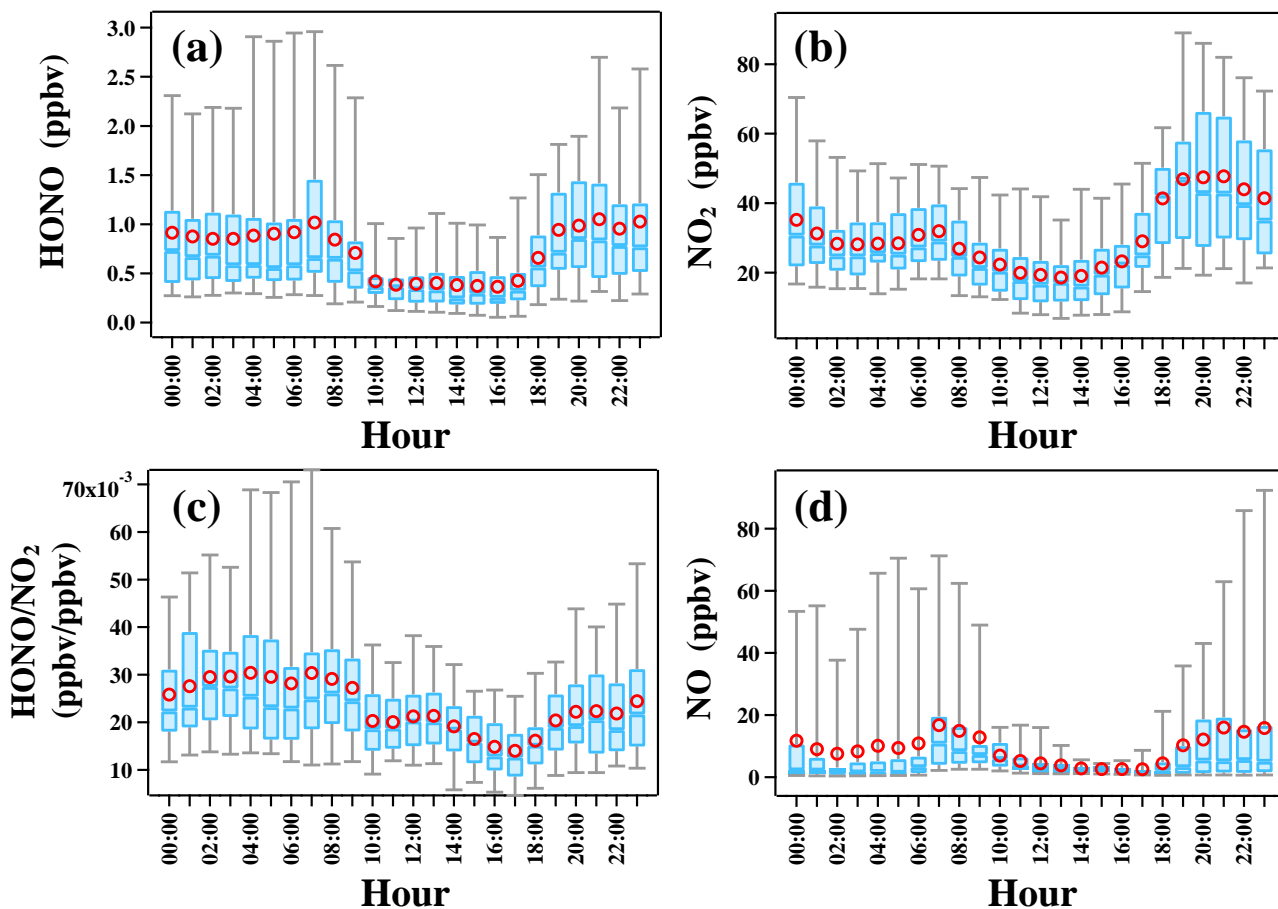


Figure 2. Diurnal profiles of HONO, NO₂, NO and HONO/NO₂ during the observation period. The blue line in the box and red circle refer to the median and mean, respectively. Boxes represent 25% to 75% of the data, and whiskers 95% of the data. The box plots presented in this study is generated by an Igor Pro-based computer program, Histbox (Wu et al., 2018).

3.2 Nocturnal HONO formation and sources

3.2.1 Direct emissions

As noted in Sect. 1, the site was expected to receive substantial direct emission of HONO from two major roads nearby. We obtained the emitted HONO/NO_x ratios in fresh plumes defined with the following criteria (Xu et al., 2015):

- (a) NO_x > 49.7 ppbv (highest 25% of NO_x data);
- (b) NO/NO_x > 0.8;
- (c) good correlation between NO_x and HONO ($R^2 > 0.70$, $P < 0.05$);

(d) short duration of plumes (< 2 h);

(e) global radiation $< 10 \text{ W m}^{-2}$ ($J(\text{NO}_2) < 0.25 \times 10^{-3} \text{ s}^{-1}$).

During the campaign, 11 fresh plumes were identified to satisfy criteria (a)–(e) (see Table S3). Two cases among them are shown in Fig. S4. The HONO/NO_x ratios in these selected plumes varied from 0.1% to 1.5% with an average value of $0.9 \pm$
235 0.4%, which is comparable to the average value of 1.2% measured in Hong Kong (Xu et al., 2015), 1.0% observed in Hong Kong (Yun et al., 2017), 0.79% measured in Nanjing (Liu et al., 2019b) and 0.69% observed in Changzhou (Shi et al., 2020b). It should be noted that the emission factor derived in this study is based on field observation and the screening criterion for fresh air mass is NO/NO_x > 0.8 , while the fresh air mass was characterized by NO/NO_x > 0.9 in the tunnel experiments conducted by Kurtenbach et al. (2001), so the air masses we selected were still slightly aged and the emission
240 factor derived in this study is slightly overestimated.

To evaluate the primary emission, three methods have been used in previous studies (Liu et al., 2019b; Liu et al., 2020b; Meng et al., 2020). In method (1), [HONO_{emis}] (the primary emission's contribution to HONO concentration) is equal to the product of emission coefficient K and observed NO_x concentration (Cui et al., 2018; Huang et al., 2017) (see Eq. (2)). This
245 method ignores the sink of NO_x and HONO, as well as transport and convection. On this basis, the observed NO_x is equal to the accumulation of NO_x emission, and HONO emission is linearly related to NO_x concentration. However, ubiquitous loss of NO_x would increase the uncertainty of this method, especially during daytime. In method (2), primary emission rate P_{emis} is equal to the product of emission coefficient K and [ΔNO_x], the increase of NO_x concentration during Δt (Liu et al., 2019b; Zheng et al., 2020) (see Eq. (3)). The promise of this method is similar to method (1), and it can only be used when NO_x is
250 increasing. As expected, a decrease in NO_x would yield a negative HONO emission rate, which is unrealistic. In method (3), P_{emis} is equal to the product of emission coefficient K and NO_x^{*}, the NO_x emission from source emission inventory (Michoud et al., 2014; Su et al., 2008b) (see Eq. (4)). This method adheres to the definition of HONO emission rate, assuming that the primary sources are evenly mixed in a specific area. It is desirable that emission inventory data with high spatial and temporal resolution are used to obtain an accurate estimate.

255

$$[\text{HONO}_{\text{emis}}] = K \times [\text{NO}_x] \quad (2)$$

$$P_{\text{emis}} = K \times [\Delta\text{NO}_x] \quad (3)$$

$$P_{\text{emis}} = K \times \text{NO}_x^* \quad (4)$$

$$P_{\text{HONO}} = \frac{[\text{HONO}]_{t_2} - [\text{HONO}]_{t_1}}{t_2 - t_1} \quad (5)$$

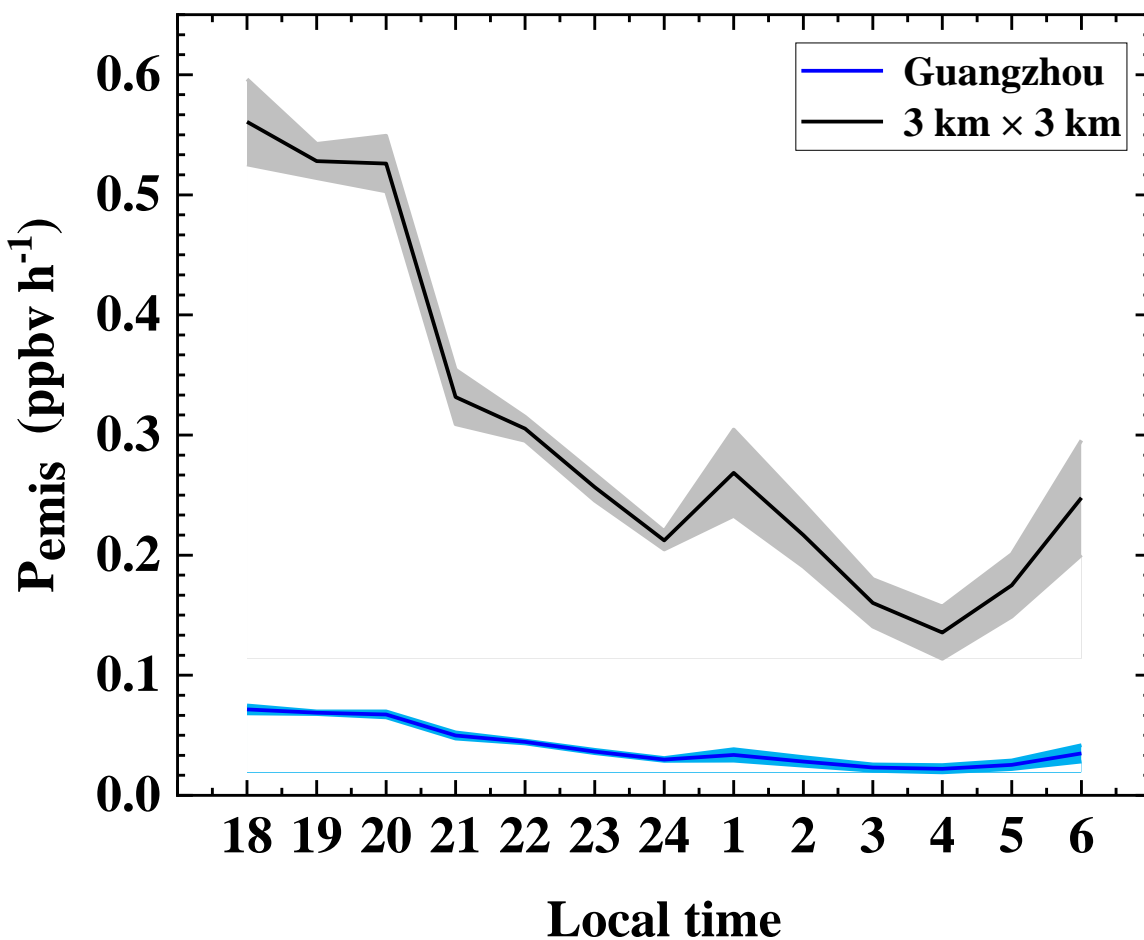
260

In this study, we first used NO_x emission rate from a high-resolution emission inventory (Huang et al., 2021) to calculate emission rate of HONO P_{emis} at night (18:00–6:00). The NO_x emission rate was extracted from a 3 km × 3 km grid cell centred around our site. As a comparison, we also used the 2017 NO_x emission inventory of Guangzhou city to repeat the

265 calculation. The two inventories are primarily different in spatial resolution. The high-resolution $3 \text{ km} \times 3 \text{ km}$ data is expected to better represent local traffic emissions, whereas the city-level emission inventory represents the total emission. Since we cannot quantify the relative contribution of the local and regional emissions to this site, two results are used to represent upper and lower limits of the contribution of primary emissions to HONO. The nighttime height of the boundary layer is assuming to 200 m according to the previous study by Fan et al. (2008).

270 The observed HONO production/accumulation rate P_{HONO} is calculated by Eq. (5), where $[\text{HONO}]_{\text{t1}}$ and $[\text{HONO}]_{\text{t2}}$ represent the HONO concentration at 18:00 and 6:00 Local Time, respectively. Then an average P_{HONO} of 0.02 ppbv h^{-1} can be derived. Hourly HONO primary emission rates calculated with the two inventories are shown in Fig. 3. P_{emis} calculated with the high-resolution emission data ($3 \text{ km} \times 3 \text{ km}$) shows a steep downward trend from 18:00 (0.56 ppbv h^{-1}) to 4:00 (0.14 ppbv h^{-1}), followed by an upward trend from 4:00 (0.14 ppbv h^{-1}) to 6:00 (0.25 ppbv h^{-1}). The average of P_{emis} is $0.30 \pm 0.15 \text{ ppbv h}^{-1}$,
275 far larger than the average accumulating rate of HONO at night (0.02 ppbv h^{-1}) derived from observed HONO variation. By contrast, P_{emis} with the city level emission data (Guangzhou) is much lower ($0.04 \pm 0.02 \text{ ppbv h}^{-1}$) and varied smoothly throughout the night. Similar results have been obtained at urban sites (Liu et al., 2020b; Liu et al., 2020c) and a suburban site (Michoud et al., 2014), while the result at a rural site is much lower (Su et al., 2008b). The lower limit of the calculated P_{emis} is still larger than the observed HONO accumulation rate. Considering the uncertainty of the inventories (-25%–28%),
280 P_{emis} may be overestimated or underestimated to the same extent. Nevertheless, direct emission of HONO is still a large HONO source at night along with other sources of HONO that remain to be considered. Furthermore, a large sink of HONO was necessary to explain the observed trend of HONO.

285



290 **Figure 3.** The nocturnal variation of HONO primary emission rates. The black and blue lines represent the HONO primary emission rates calculated by the 2017 NO_x emission source inventory of the 3 km × 3 km grid cell centred on the Guangzhou Institute of Geochemistry and the 2017 NO_x emission source inventory of Guangzhou city respectively. The coloured areas represent 1 – σ standard deviations.

Method (1) is also adopted here to calculate [HONO]_{emis}, and [HONO]_{emis}/[HONO] can simply represent the primary emission's contribution to HONO. We summarized [HONO]_{emis}/[HONO] ratios obtained from urban sites in China (Table S4). The values varied at a wide range from 12% to 52%, and the difference of 2 times or more existed in different seasons at the same site. These indicate the complexity of the impact of source emissions on observation site. The ratio of [HONO]_{emis}/[HONO] at our site is at a high level of 47%, indicating that the site during the campaign is more strongly affected by primary emission from vehicle exhaust compared to most previous studies.

In addition to traffic emissions, we also estimated the HONO emission rate from soil P_{soil} (ppbv h^{-1}) according to Eq. (6):

$$300 \quad P_{\text{soil}} = \frac{\alpha F_{\text{soil}}}{H} \quad (6)$$

where F_{soil} is the emission flux ($\text{g m}^{-2} \text{s}^{-1}$); H is the height of boundary layer (H , m) and was assumed to be 200 m (Fan et al., 2008); α is the conversion factor ($\alpha = \frac{1 \times 10^9 \times 3600 \times R \times T}{M \times P} = \frac{2.99 \times 10^{13} \times T}{M \times P}$); T is the temperature (K); M is the molecular weight (g mol^{-1}) and P is the atmospheric pressure (Pa). HONO emission flux from soil depends on the temperature, water content and nitrogen nutrient content of soil, which have been considered according to the parameters reported in the literature (Oswald et al., 2013). Since grassland, coniferous forest and tropical rain forest are the typical plants in Guangzhou city area (Wu et al., 2015) and their emission fluxes are comparable (Oswald et al., 2013), emission flux from grassland was adopted to represent the soil HONO emission in Guangzhou. The average nighttime P_{soil} varied from 0.011 to 0.035 ppbv h^{-1} , with a mean value of 0.019 ± 0.001 ppbv h^{-1} . It is comparable to the lower limit of primary emission rate of 0.04 ± 0.02 ppbv h^{-1} .

3.2.2 NO + OH homogeneous reaction

310 The reaction between NO and OH acts as the principle homogenous HONO source. It can contribute a substantial fraction to HONO formation when NO and OH concentrations are high (Alicke et al., 2003; Liu et al., 2019b; Wong et al., 2011; Tong et al., 2015). Taking the homogeneous Reactions R2 and R3 into account, the net HONO homogeneous production rate can be calculated by following Eq. (7):

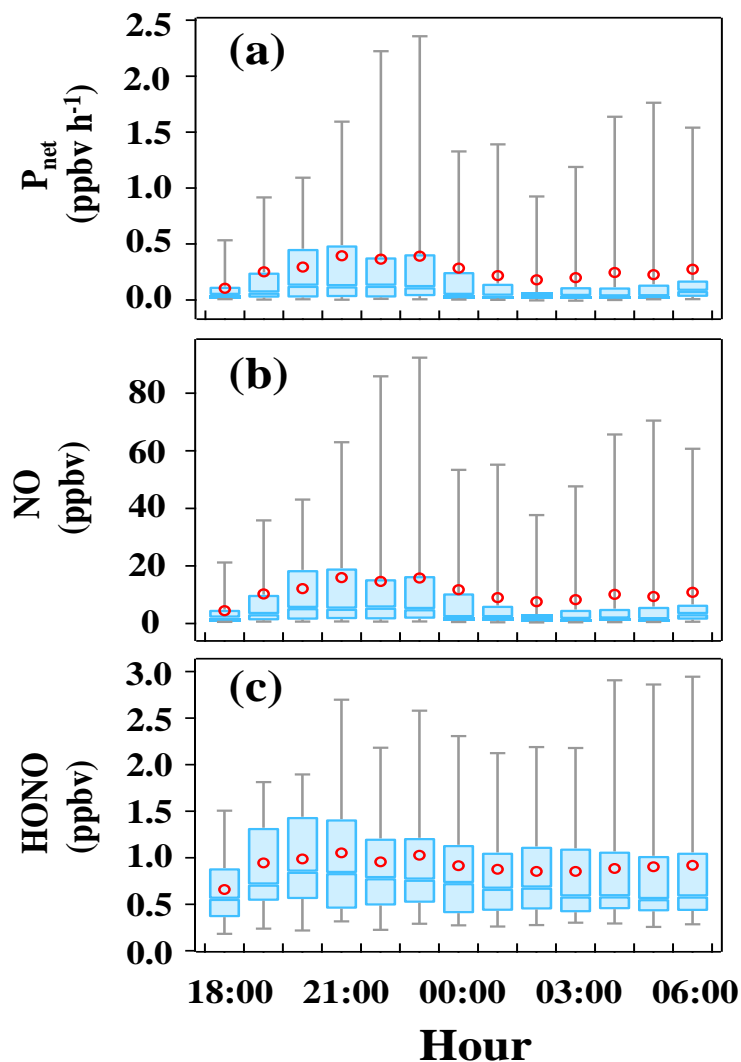


$$P_{\text{net}} = k_{\text{NO+OH}}[\text{NO}][\text{OH}] - k_{\text{HONO+OH}}[\text{HONO}][\text{OH}] \quad (7)$$

In Eq. (7), $k_{\text{NO+OH}}$ ($7.2 \times 10^{-12} \text{ cm}^3 \text{ s}^{-1}$) and $k_{\text{HONO+OH}}$ ($5.0 \times 10^{-12} \text{ cm}^3 \text{ s}^{-1}$) are the reaction rate constants of the Reactions R2 and R3 at 298 K, respectively (Li et al., 2012). Since the OH concentration was not measured, an average nighttime value of $1.0 \times 10^6 \text{ cm}^{-3}$ measured in Heshan in the PRD region in autumn of 2014 was assumed (Liu, 2017). As shown in Fig. 4, the variation of P_{net} is highly similar to NO, for the concentration of NO was 10 times larger than HONO. And the average value of P_{net} is 0.26 ± 0.08 ppbv h^{-1} , leading to a cumulative HONO contribution of 3.24 ppbv. However, the measured HONO only increased 0.26 ppbv in this period. It suggests that, (1) the reaction between NO and OH is adequate to explain the HONO increase in the whole night, even though other sources like NO_2 heterogeneous conversion might still exist; (2) except for HONO + OH, the strength of HONO sink should be at least 0.30 ppbv h^{-1} , 6 times larger than that obtained by Li et al. (2012) and comparable to that by Hao et al. (2020).

We carried out sensitivity tests using one tenth, twice and half of assumed OH concentration ($1.0 \times 10^6 \text{ cm}^{-3}$) (Lou et al., 2010). As is shown in Table S5, within the range of nighttime OH concentration, the cumulative production of the

homogeneous reaction of $\text{NO} + \text{OH}$ in this study are all larger than the averaged measured accumulation of HONO, indicating that taking a value within the range of the observed nighttime OH concentration will not affect the conclusion of this study.



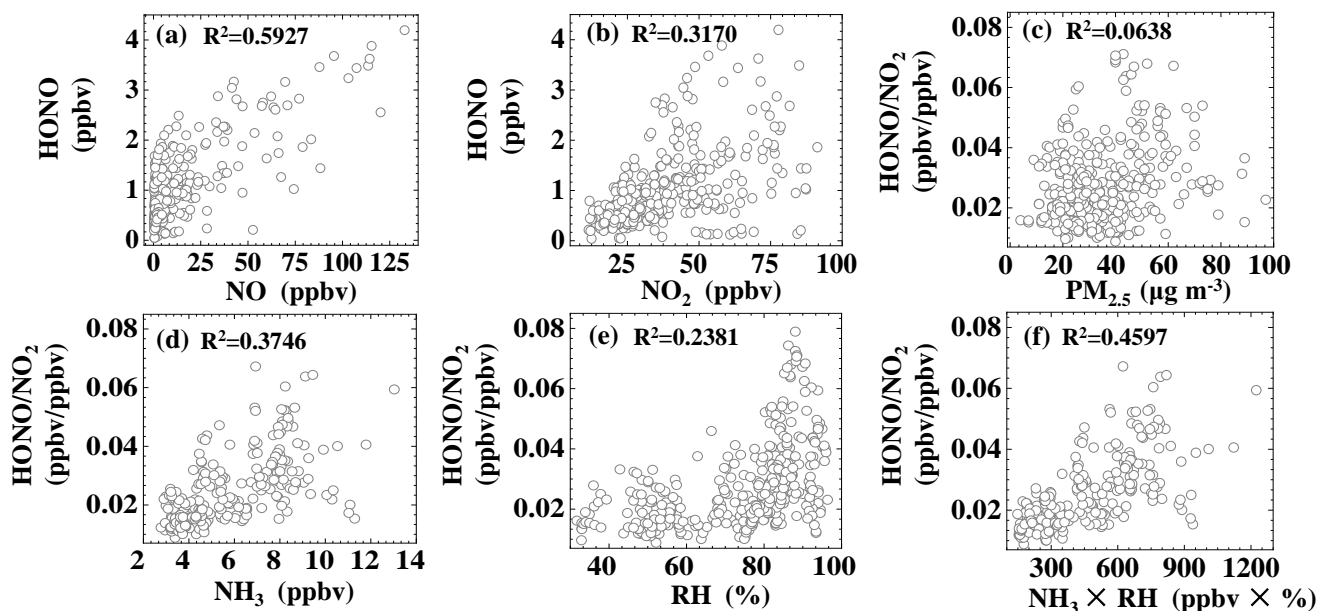
335 **Figure 4.** The mean nocturnal variation of P_{net} , HONO and NO. The blue line in the box and red circle refer to the median and mean, respectively. Boxes represent 25% to 75% of the data, and whiskers 95 % of the data.

3.2.3 NO_2 to HONO heterogeneous conversion

Our analysis so far suggests that direct emissions and the homogeneous reaction between NO and OH are more than sufficient to explain the growth of HONO concentration through the night. The relatively high correlation ($R^2 = 0.5927$)

340 between HONO and NO is in line with this finding (Fig. 5 (a)). In addition, correlation analysis was conducted to explore possible pathways of heterogeneous NO₂ to HONO conversion at night (18:00–6:00).

The ratio of HONO/NO₂ has often been used to indicate the heterogeneous conversion efficiency of NO₂ to HONO (Lammel and Cape, 1996; Stutz et al., 2002), for being less influenced by transport processes or convection. Figure 5 (c) shows a weak correlation ($R^2 = 0.0638$) between HONO/NO₂ and PM_{2.5}, suggesting that the formation of HONO on aerosol surfaces might not be the main pathway (Kalberer et al., 1999; Kleffmann et al., 2003; Wong et al., 2011; Zhang et al., 2009; Sörgel et al., 2011a; VandenBoer et al., 2013). Because the surface area of ground (including vegetation surface, building surface and soil, etc.) is generally larger than the surface area of aerosols (Zhang et al., 2016), some studies suggested that the heterogeneous reaction of NO₂ and water vapor on ground surfaces was the main source of HONO (Harrison and Kitto, 1994; Li et al., 2012; Wong et al., 2012). Furthermore, the correlations between HONO/NO₂ and NH₃ and RH are 0.3746 and 0.2381, respectively, and the correlation further improved between HONO/NO₂ and the product of NH₃ and RH ($R^2 = 0.4597$). Some studies proposed that NH₃ can decrease the free-energy barrier in hydrolysis of NO₂ thus enhance the HONO formation (Xu et al., 2019; Li et al., 2018b; Zhang and Tao, 2010; Wang et al., 2021).



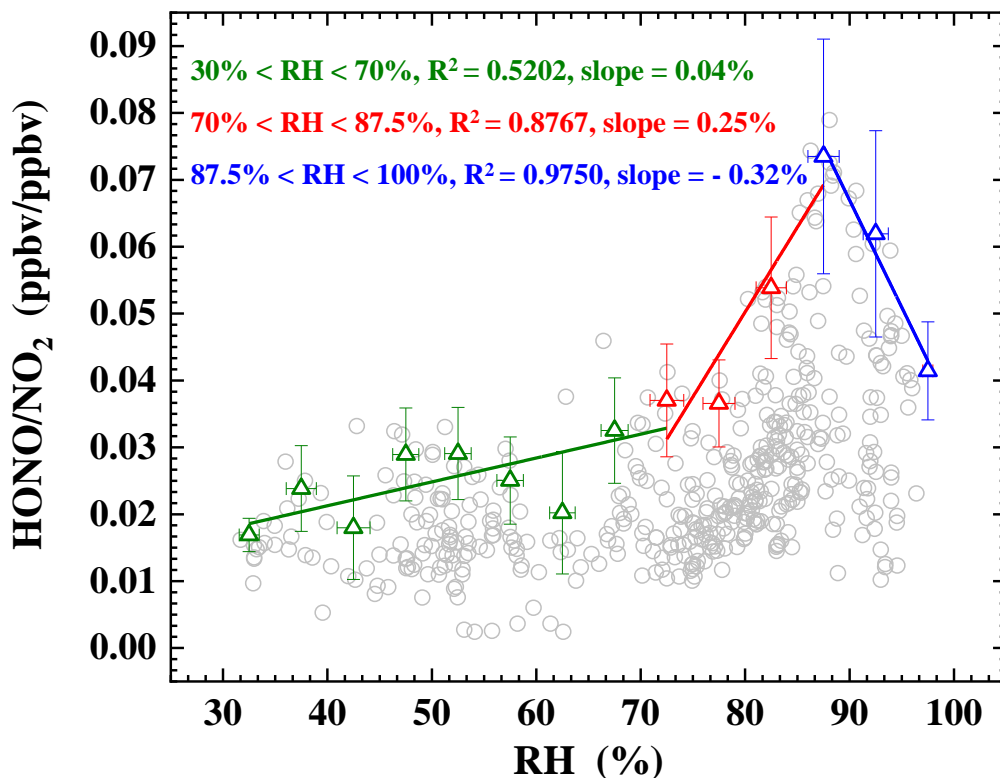
355 **Figure 5. Correlations between HONO, HONO/NO₂ and various parameters during the time interval of 18:00–6:00.**

In Fig. 6, we further explored the RH effect by focusing on high HONO/NO₂ values, i.e., the 5 highest HONO/NO₂ values for 5% RH intervals (Stutz et al., 2004). When RH was lower than 87.5%, HONO/NO₂ increased with RH, which is in accordance with the reaction kinetics of disproportionation reaction of NO₂ and H₂O. Furthermore, the slope of linear fitting between HONO/NO₂ and RH was much smaller for RH range of 30% ~ 70% (slope = 0.04%; $R^2 = 0.5202$) than for the RH range of 70% ~ 87.5% (slope = 0.25 %, $R^2 = 0.8767$). Similar piecewise correlations between HONO/NO₂ and RH have been

found in previous studies (Qin et al., 2009; Zhang et al., 2019b), which have been interpreted as evidence for the non-linear dependence of NO₂-to-HONO conversion efficiency on RH. Once the relative humidity exceeded 87.5%, NO₂-to-HONO conversion appeared to be inhibited by RH (slope = - 0.32%; R² = 0.9750). A possible explanation is that the number of water layers formed on various surfaces increased rapidly with RH, resulting in effective uptake of HONO and making the surface inaccessible or less reactive to NO₂. Previous studies also found fast growth of aqueous layers when RH over 70% for glass (Saliba et al., 2001) and over 80% for stone (Stutz et al., 2004). The tipping point inferred from ambient observations appear to vary across locales, likely reflecting the different composition of the ground surfaces, e.g., 60% for Chengdu (Yang et al., 2021c), 65–70% for Beijing (Wang et al., 2017a), 70% for Back Garden (Li et al., 2012), 75% for Shanghai (Wang et al., 2013), and 85% for Xi'an (Huang et al., 2017).

370

In sum, our correlation analysis for HONO/NO₂ suggests that nighttime heterogenous conversion of NO₂ into HONO at our site might be related to NH₃ and water vapor, whereas aerosol surfaces appeared unimportant.



375 Figure 6. Scatter plot of HONO/NO₂ ratio against RH during nighttime from 18:00 to 6:00. Triangles are the average of top-5 HONO/NO₂ values in each 5% RH interval.

3.2.4 Removal of HONO through dry deposition

As discussed in Sect. 3.2.2, a sink of at least 0.30 ppbv h⁻¹ is required to balance the nighttime HONO production. Since the reactions of HONO + OH and HONO + HONO are negligible (Kaiser and Wu, 1977; Mebel et al., 1998), it is conceivable that HONO is mainly removed through deposition on the ground. HONO dry deposition velocity V_d can be estimated with

380 Eq. (8):

$$\frac{d[\text{HONO}]}{dt} = P_{\text{emis}} + P_{\text{soil}} + P_{\text{net}} - \frac{V_d \times [\text{HONO}]}{H} \quad (8)$$

The average deposition velocity V_d between 18:00–6:00 was calculated to be 1.8 cm s⁻¹, which is within the range of prior researches (0.077–3 cm s⁻¹) (Harrison and Kitto, 1994; Harrison et al., 1996; Stutz et al., 2002; Li et al., 2012; Spindler et al.,
385 1999), and also consistent to the results derived from the HONO uptake coefficient on soil and ground (Donaldson et al., 2014; VandenBoer et al., 2013). It should be noted that heterogeneous conversion of NO₂-HONO has not been taken into account, so 1.8 cm s⁻¹ is the lower limit of dry deposition velocity. High RH at night probably increased the amount of adsorbed water on the ground surfaces and facilitates dry deposition of HONO.

390 In sum, primary emission from vehicle exhaust (between 0.04 ± 0.02 ppbv h⁻¹ and 0.30 ± 0.15 ppbv h⁻¹) and the homogeneous reaction of OH + NO (0.26 ± 0.08 ppbv h⁻¹) were major sources of HONO at night. Nighttime soil emission rate was calculated to be 0.019 ± 0.001 ppbv h⁻¹, which is comparable to the observed nocturnal increase rate of HONO (0.02 ppbv h⁻¹), further indicating the importance of direct emissions. Additionally, contribution from NO₂ heterogeneous reactions on surfaces should not be ruled out. To balance the nighttime HONO budget by assuming dry deposition to be the
395 principal loss process, a dry deposition rate of at least 1.8 cm s⁻¹ is required.

3.3 Daytime HONO budget and unknown sources analysis

In this section, we concentrate on the daytime chemistry of HONO by a detailed budget analysis. The time variation of HONO concentration at our site can be related to its sources and sinks as follows:

400

$$\frac{\partial[\text{HONO}]}{\partial t} = P_{\text{HONO}} - L_{\text{HONO}} = (P_{\text{OH+NO}} + P_{\text{Unknown}} + P_{\text{emis}} + P_{\text{soil}} + T_V + T_H) - (L_{\text{OH+HONO}} + L_{\text{Phot}} + L_{\text{Dep}}) \quad (9)$$

where ∂[HONO]/∂t represents the time variation of HONO; P_{HONO} and L_{HONO} are the sources and sinks of HONO, respectively; P_{OH+NO} and L_{OH+HONO} are the homogeneous HONO formation and loss rates in Reactions R2 and R3,
405 respectively; P_{Unknown} is the HONO production rate from unknown sources; T_V and T_H are two terms representing vertical and horizontal transport processes, respectively; L_{Phot} denotes the photolysis loss rate of HONO, which can be calculated

with $L_{\text{Phot}} = J(\text{HONO}) \times [\text{HONO}]$; L_{Dep} represents the deposition loss rate of HONO and can be calculated as $L_{\text{Dep}} = V_d \times [\text{HONO}]/H$, where V_d is the deposition velocity of HONO and H is the daytime mixing height. Assuming a daytime V_d of 1.6 cm s^{-1} (Hou et al., 2016; Li et al., 2011) and an daytime mixing height (H) of 1000 m (Liao et al., 2018; Song et al., 2019), the average L_{Dep} is $0.003 \pm 0.001 \text{ ppbv h}^{-1}$, three orders of magnitude smaller than L_{Phot} and therefore can be ignored in the following discussion.

OH was not measured and was calculated with a parameterized approach based on strong correlation between observed OH radicals and $J(\text{O}^1\text{D})$. The parameterization was first proposed by Rohrer and Berresheim (2006) and has been applied by several studies in China (Lu et al., 2013; Lu et al., 2012; Lu et al., 2014). In this study, OH was estimated with observed $J(\text{O}^1\text{D})$ along with parameters from fitting the observed OH radicals and $J(\text{O}^1\text{D})$ data in Guangzhou Back Garden by Lu et al. (2012). The daytime maximum OH concentration was estimated to be $1.3 \times 10^7 \text{ cm}^{-3}$, which is slightly smaller than the daily peak values of $1.5\text{--}2.6 \times 10^7 \text{ cm}^{-3}$ observed in summer of Guangzhou by Lu et al. (2012). And the estimated daily average OH concentration is $6.7 \times 10^6 \text{ cm}^{-3}$, close to $7.5 \times 10^6 \text{ cm}^{-3}$ measured in the PRD region in autumn of 2014 by Yang et al. (2017b). Daytime P_{emis} was calculated based on the method (3) (mentioned in Sect. 3.2.1). Because the HONO lifetime was in the order of 20 min under typical daytime conditions (Stutz et al., 2000) and the transport distance is only a few kilometers, the NOx emission rate extracted from the $3 \text{ km} \times 3 \text{ km}$ grid cell centred around sampling site is used to calculate the impact of primary emission on HONO.

To minimize interferences, we choose a period from 9:00 to 15:00 with intense solar radiation and a short HONO lifetime. Horizontal transport T_H was assumed negligible by selecting the cases with low wind speed (Su et al., 2008b; Yang et al., 2014). The magnitude of vertical transport T_V can be estimated by using a parameterization for dilution by background air according to (Dillon et al., 2002), i.e. $T_V = k_{(\text{dilution})} \times ([\text{HONO}] - [\text{HONO}]_{\text{background}})$. Where $k_{(\text{dilution})}$ is the dilution rate, $[\text{HONO}]_{\text{background}}$ represents the background HONO concentration. Assuming a $k_{(\text{dilution})}$ of 0.23 h^{-1} (Dillon et al., 2002; Sörgel et al., 2011a), a $[\text{HONO}]_{\text{background}}$ value of 10 pptv (Zhang et al., 2009), and taking the mean noontime $[\text{HONO}]$ value of 400 pptv in this study, a value of about 0.09 ppbv h^{-1} can be derived, which is much smaller than L_{Phot} and can be ignored in the following discussion. The average daytime HONO emission rate from soil P_{soil} varied from 0.002 to 0.007 with a mean value of $0.004 \pm 0.001 \text{ ppbv h}^{-1}$, which is three orders of magnitude smaller than L_{Phot} , and can also be ignored in the following discussion. As a result, P_{Unknown} can be expressed by Eq. (10), in which $\partial[\text{HONO}]/\partial t$ is substituted by $\Delta[\text{HONO}]/\Delta t$.

435

$$\frac{\Delta[\text{HONO}]}{\Delta t} = (P_{\text{OH+NO}} + P_{\text{emis}} + P_{\text{Unknown}}) - (L_{\text{OH+HONO}} + L_{\text{Phot}}) \quad (10)$$

Figure 7 shows the budget of HONO from 9:00 to 15:00. As expected, photolysis HONO L_{Phot} ($1.58 \pm 0.82 \text{ ppbv h}^{-1}$) is the main loss pathway in the day, followed by a small contribution by the homogeneous reaction of HONO + OH ($L_{\text{OH+HONO}}$,

440 $0.07 \pm 0.03 \text{ ppbv h}^{-1}$). Among the sources, $P_{\text{OH+NO}}$ and P_{Unknown} were comparable in magnitudes, with an average of $0.79 \pm$
 0.61 ppbv h^{-1} and $0.65 \pm 0.46 \text{ ppbv h}^{-1}$, respectively. P_{Unknown} showed a photo-enhanced feature, reaching its maximum at
 12:00 at 0.97 ppbv h^{-1} , similar to the observations in Xinken (Su et al., 2008b), Beijing (Yang et al., 2014), Wangdu (Liu et
 al., 2019a), Changzhou (Zheng et al., 2020) and Cyprus (Meusel et al., 2016). The average of P_{Unknown} is comparable to the
 observation in Back Garden (0.77 ppbv h^{-1}) by Li et al. (2012), but smaller than those in Xinken ($\approx 2.0 \text{ ppbv h}^{-1}$) by Su et al.
 445 (2008b) and Guangzhou city area (1.25 ppbv h^{-1}) by Yang et al. (2017a). Homogeneous reaction of $\text{NO} + \text{OH}$ reached its
 maximum in the early morning, and contributed the most fraction in the whole day. Apparently, high NO concentrations at
 our site made $P_{\text{OH+NO}}$ the biggest daytime source of HONO, exceeding P_{Unknown} , similar to other high-NO_x sites such as
 Santiago de Chile (Elshorbany et al., 2009), London (Heard et al., 2004), Paris (Michoud et al., 2014), Beijing (Liu et al.,
 2021; Slater et al., 2020; Zhang et al., 2019b; Liu et al., 2020c), Taiwan (Lin et al., 2006) and Hebei (Xue et al., 2020). Next,
 450 we investigate possible factors relating to P_{Unknown} .

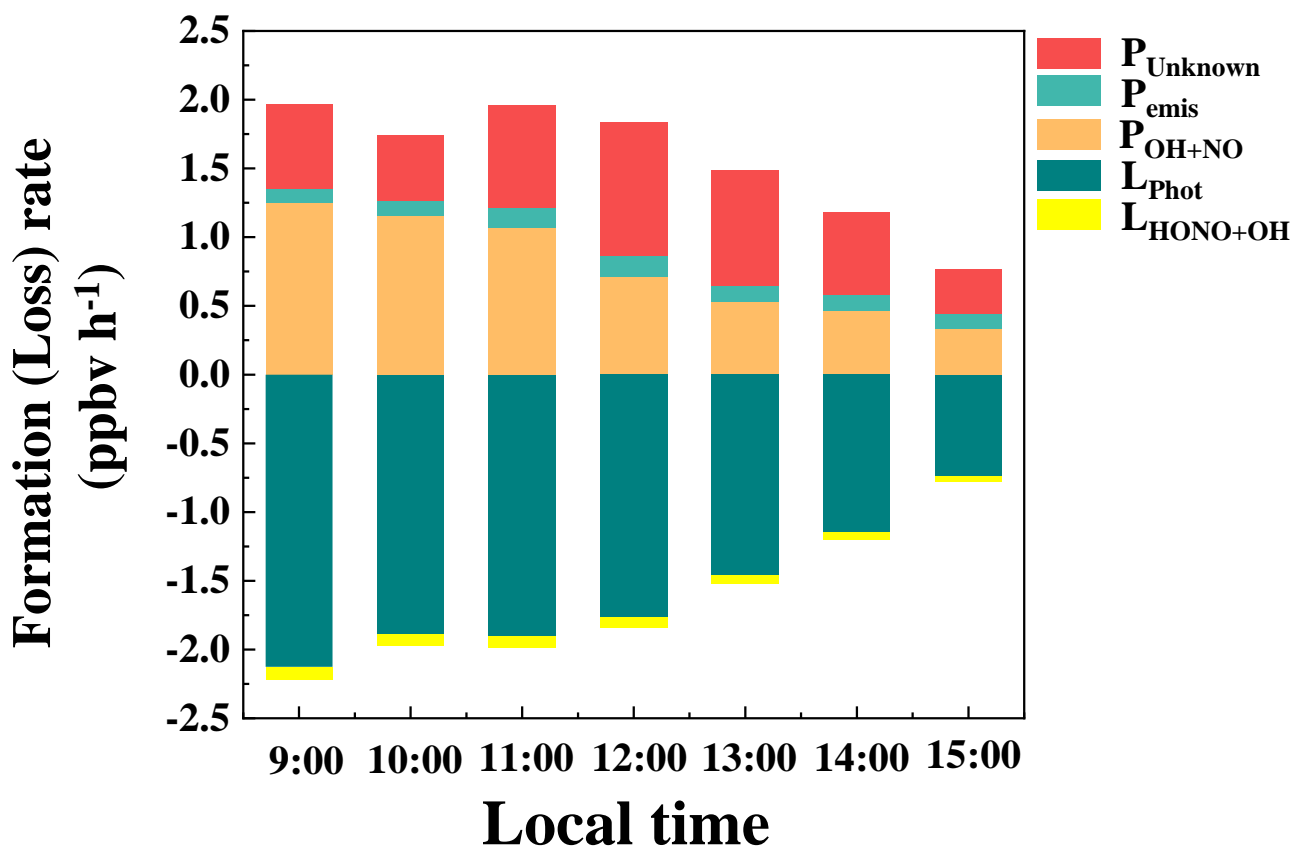


Figure 7. Items of the HONO budget (Eq. (10)) in Guangzhou during the observation period.

Figure 8 shows the correlation between P_{Unknown} and NO_2 and $J(\text{NO}_2)$ was 0.0681 and 0.2713, respectively. The correlation between P_{Unknown} and $\text{NO}_2 \times J(\text{NO}_2)$ further improved to 0.4116, indicating that P_{Unknown} may be related to the photo-

455 enhanced reaction of NO₂ (Jiang et al., 2020; Li et al., 2018a; Liu et al., 2019a; Liu et al., 2019b; Su et al., 2008b; Zheng et al., 2020; Huang et al., 2017).

No correlation was found between P_{Unknown} and PM_{2.5} ($R^2 = 0.00014$), indicating that particulate matters may not be a key factor in daytime HONO production (Wong et al., 2012; Li et al., 2018a; Sörgel et al., 2011a; Wang et al., 2017a; Zheng et al., 2020). Meanwhile, the correlations between P_{Unknown} and nitrate in PM₁ and the sum of gaseous nitric acid and nitrate in PM₁ were very low, with R^2 of 0.0348 and 0.0062 respectively. And the correlation between P_{Unknown} and the product of nitrate and J(NO₂) was also poor $R^2 = 0.0007$, which does not relate P_{Unknown} to the photolysis of nitrate or gaseous nitric acid. Wang et al. (2016) and Ge et al. (2019) suggested that NH₃ can efficiently promote the reaction of NO₂ and SO₂ to form HONO and sulfate. However, we did not find good correlations for P_{Unknown} vs. NH₃, P_{Unknown} vs. SO₂, or P_{Unknown} vs. NH₃ × SO₂.

In summary, at our site with relatively strong traffic impact and high NO, NO + OH appears to be the largest daytime HONO source followed by an unknown photolytic source, which does not seem to be related to aerosols, nor the photolysis of nitrate/nitric acid, nor the reaction between NO₂, SO₂ and NH₃.

470

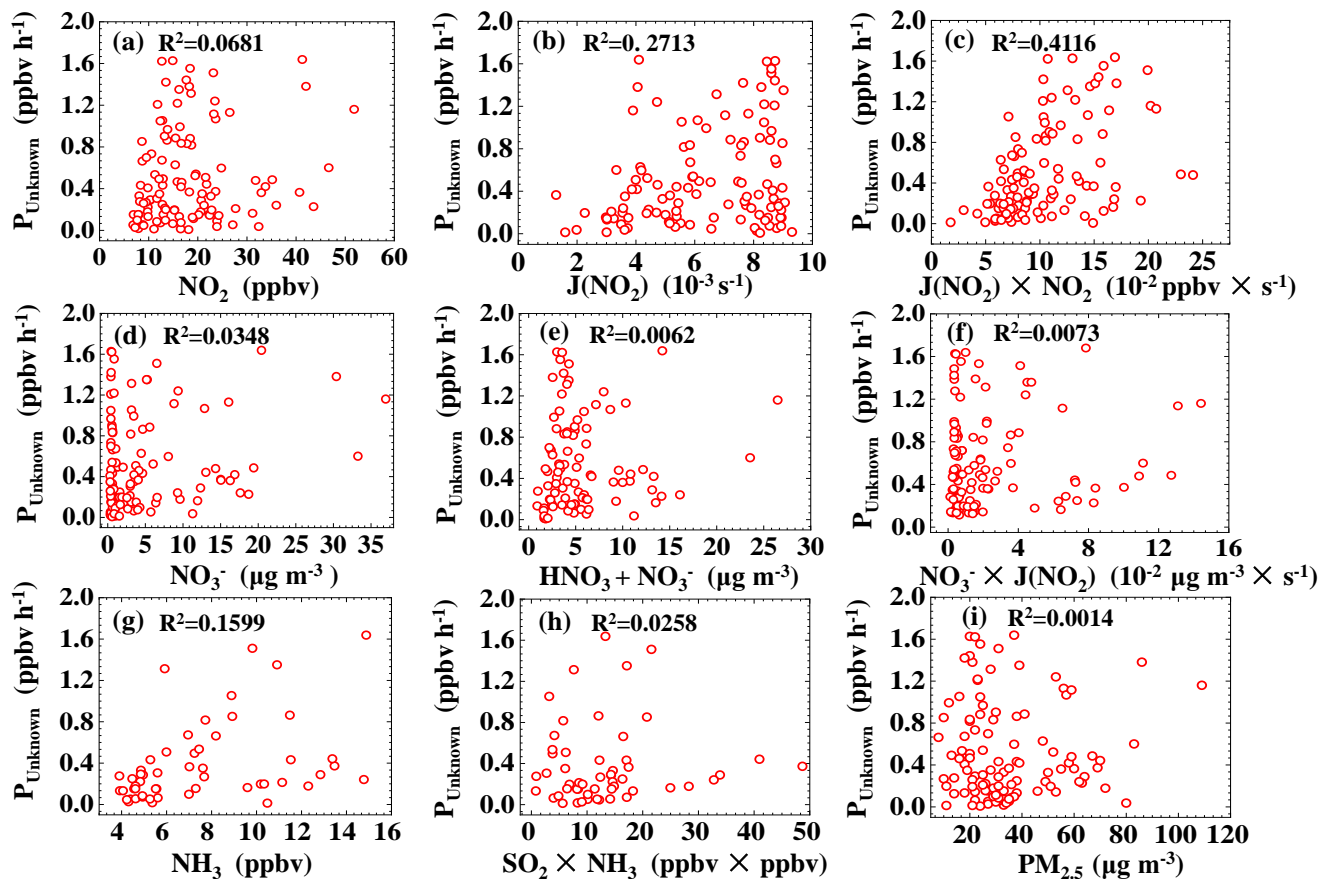


Figure 8. Correlations between daytime HONO unknown sources P_{Unknown} and related parameters.

3.4 The contribution of HONO, O_3 and ozonolysis of alkenes to OH

Photolysis of HONO and O_3 contribute dominant the primary source of OH radicals. Ozonolysis of alkenes was found to be
 475 important source of OH (Heard et al., 2004; Elshorbany et al., 2009; Tan et al., 2019b). Here we evaluated and compared the
 contribution of the three pathways. Other sources such as the photolysis of peroxides, is usually not very significant in urban
 areas, especially during daytime, thus was not considered in this study (Li et al., 2018a; Shi et al., 2020b). The contribution
 of HCHO photolysis to OH was also not considered due to the lack of measurement for HCHO. The OH radicals' production
 rate from HONO photolysis $P_{\text{OH(HONO)}}$ can be calculated from the measured photolysis frequencies and the mixing ratios of
 480 HONO using Eq. (11). The net OH radicals' production from HONO $P_{\text{(HONO-OH)}}$ can be calculated by subtracting the OH
 loss caused by Reactions R1 and R2 from $P_{\text{OH(HONO)}}$ (Eq. (12)). The OH radicals' production rate from O_3 photolysis $P_{\text{(O}_3\text{-OH)}}$
 can be calculated from Eq. (13). Only part of $O(^1D)$ atoms, formed through the photolysis of O_3 at solar radiation below 320
 nm (Reaction R4), can generate OH radicals by reacting with water vapor (Reaction R5) in the atmosphere, so we used the
 absolute mixing ratio of water vapor, which can be derived from the temperature and relative humidity data, to calculate the

485 fraction of OH (Φ_{OH}) between Reactions R5 and R6. The reaction rate of $\text{O}(^1\text{D})$ with N_2 and O_2 is $3.1 \times 10^{-11} \text{ cm}^3 \text{ s}^{-1}$ and $4.0 \times 10^{-11} \text{ cm}^3 \text{ s}^{-1}$ respectively (Seinfeld and Pandis, 2016). In Eq. (15), $k_{\text{alkenes}(i)+\text{O}_3}$ represents the reaction rate constant for the reaction of O_3 with alkene (i), and Y_{OH_i} represents the yield of OH from the gas-phase reaction of O_3 and alkene (i). Table S6 summarized the reaction rate constant of O_3 with alkenes at 298 K and the yields of OH.

$$490 \quad P_{\text{OH}(\text{HONO})} = J(\text{HONO})[\text{HONO}] \quad (11)$$

$$P_{(\text{HONO}-\text{OH})} = P_{\text{OH}(\text{HONO})} - k_{\text{NO}+\text{OH}}[\text{NO}][\text{OH}] - k_{\text{HONO}+\text{OH}}[\text{HONO}][\text{OH}] \quad (12)$$

$$P_{(\text{O}_3-\text{OH})} = 2\Phi_{\text{OH}}[\text{O}_3]J(\text{O}^1\text{D}) \quad (13)$$

$$\Phi_{\text{OH}} = k_5[\text{H}_2\text{O}] / (k_5[\text{H}_2\text{O}] + k_6[\text{M}]) \quad (14)$$

$$P_{(\text{O}_3+\text{alkenes})-\text{OH}} = \sum k_{\text{alkenes}(i)+\text{O}_3}[\text{alkenes}(i)][\text{O}_3] Y_{\text{OH}_i} \quad (15)$$



Figure 9 shows that $P_{(\text{HONO}-\text{OH})}$ was larger than $P_{(\text{O}_3-\text{OH})}$ before 10:00, while the latter became always higher with the solar radiation enhanced after 10:00. Both the two sources of OH reached their maximum around 12:00, while $P_{(\text{O}_3-\text{OH})}$ was approximately two times of that of $P_{(\text{HONO}-\text{OH})}$. On average, the OH production rates by photolysis of HONO and O_3 were $3.7 \times 10^6 \text{ cm}^{-3} \text{ s}^{-1}$ and $4.9 \times 10^6 \text{ cm}^{-3} \text{ s}^{-1}$, respectively. In daytime, the sum of OH production rates by ozonolysis of alkenes was $3 \times 10^5 \text{ cm}^{-3} \text{ s}^{-1}$, which is much smaller than that of HONO and O_3 . This value ($3 \times 10^5 \text{ cm}^{-3} \text{ s}^{-1}$) was comparable to the results in previous studies (Kim et al., 2014; Ge et al., 2021; Martinez et al., 2003; Ren et al., 2003; Lee et al., 2016; Alicke et al., 2002; Kleffmann et al., 2005; Ren et al., 2013), but smaller than some other studies (Shi et al., 2020b; Zheng et al., 2020; Heard et al., 2004). Table 2 summarizes the OH production rate from HONO and O_3 photolysis from previous studies worldwide. It can be seen that $P_{(\text{HONO}-\text{OH})}$ are larger than $P_{(\text{O}_3-\text{OH})}$ in most of the observations, but sometimes the opposite is reported. Apparently, the relative importance of $P_{(\text{HONO}-\text{OH})}$ and $P_{(\text{O}_3-\text{OH})}$ strongly depends on the ratio of HONO/ O_3 . Especially in winter, photolysis of HONO tends to be the predominant OH source due to the low concentration of O_3 and water vapor.

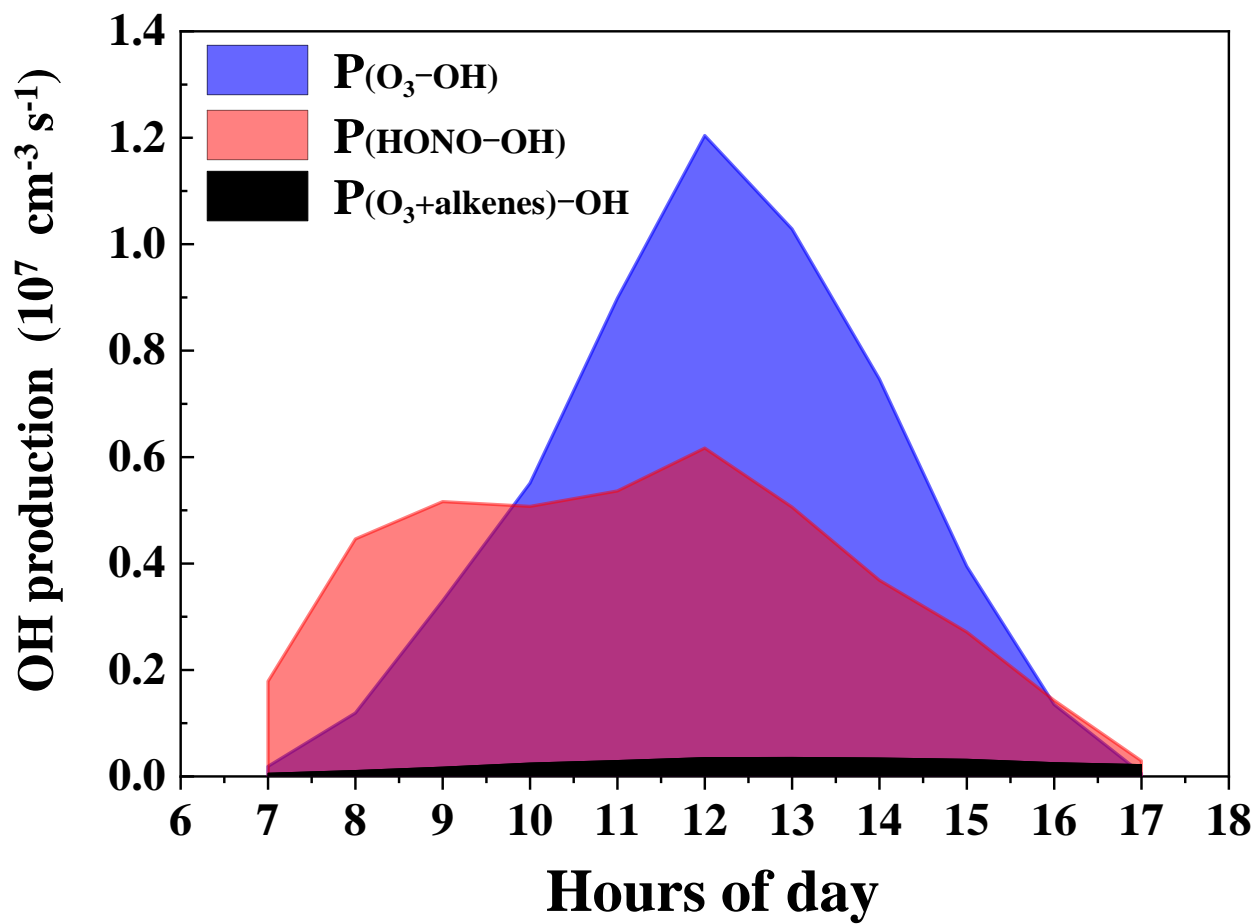


Figure 9. The yield and comparison of OH radicals by HONO, O_3 and ozonolysis of alkenes.

Table 2. The OH production rates from HONO and O₃ photolysis in previous observations.

Location	Date	Season	P _(HONO-OH) (ppbv h ⁻¹)	P _(O₃-OH) (ppbv h ⁻¹)	Reference
New York, USA	Jun–Jul 1998	Summer	0.10	0.22	1
Nashville, USA	Jun–Jul 1999	Summer	0.29	0.33	2
Birmingham, UK	Jan–Feb 2000	Winter	0.45	0.01	3
New York, USA	Jun–Aug 2001	Summer	0.81	0.19	4
Santiago, Chile	May–Jun 2005	Winter	2.90	0.01	5
	Mar 2005	Summer	1.70	0.13	
El Arenosillo, Spain	Dec 2008	Winter	0.11	0.09	6
Colorado, USA	Feb–Mar 2011	Winter	0.45	0.04	7
Beijing, China	Sep–Oct 2004	Autumn	1.31	0.18	8
Xinken, China	Oct–Nov 2004	Autumn	3.66	0.88	9
Back Garden, China	Jul 2006	Summer	1.32	2.20	10
Yufa, China	Aug 2006	Summer	1.68	0.38	11
Tung Chung, China	Aug 2011	Summer	1.50	0.90	12
Wangdu, China	Jun 2014	Summer	1.68	1.20	13
Hong Kong, China	Mar–May 2015	Spring	6.40	a	14
Changzhou, China	Dec 2015	Winter	1.04	0.36	15
	Oct 2015	Autumn	1.24	0.41	
Guangzhou, China	Jul 2016	Summer	0.71	0.44	16
	Aug 2016	Summer	1.88	0.63	
Changzhou, China	Apr 2017	Spring	1.66	2.78	18
Mount Tai, China	Dec 2017	Winter	0.52	0.02	19
	Mar–Apr 2018	Spring	0.51	0.18	
Nanjing, China	Nov–Nov 2017/2018	A year	1.16	0.41	20
Gucheng, China	Jan–Feb 2018	Winter	1.40	0.01	21
Guangzhou, China	Sep–Nov 2018	Autumn	0.54	0.72	22

515 a: far less than P_(HONO-OH).

Reference: 1. Zhou et al. (2002a); 2. Martinez et al. (2003); 3. Heard et al. (2004); 4. Ren et al. (2003); 5. Elshorbany et al. (2010); 6. Sörgel et al. (2011a); 7. Kim et al. (2014); 8. An et al. (2009); 9. Su et al. (2008b); 10. Su (2008); 11. Yang et al. (2014); 12. Xue et al. (2016); 13. Liu et al. (2019a); 14. Yun et al. (2017); 15. Zheng et al. (2020); 16. Yang et al. (2017a); 17. Li et al. (2018a); 18. Shi et al. (2020a); 19. Jiang et al. (2020); 20. Liu et al. (2019b); 21. (Li in preparation); 22. This study

520 3.5 Box model simulation of HONO impact on atmospheric oxidation capacity

Atmospheric oxidation capacity refers to the total removal rates of CO and VOCs by major oxidants (e.g., OH, NO₃ and O₃) (Elshorbany et al., 2010; Xue et al., 2016; Tan et al., 2019b). As the primary oxidant in the atmosphere, the OH concentration is widely used to quantitatively describe the atmospheric oxidation capacity (Zheng et al., 2020; Liu et al., 2021; Shi et al., 2020b; Zhang et al., 2019a). And ozone is another indicator of atmospheric oxidation capacity. A box model (MCMv3.3.1) was conducted to simulate OH and O₃ concentrations with and without HONO constrained with observational data. Figure S5 shows the time series of measured and simulated O₃ concentrations. The model performance was evaluated to be good by the index of agreement (IOA) (see Supplementary information). It should be noted that the box model ignores the influence of transport and convection, so the simulated O₃ concentration does not represent the actual O₃ concentration in the atmosphere.

530

The time series of simulation results of O₃ and OH can be found in Fig. S6. Figure 10 shows diurnal variations of simulated O₃ and OH with and without HONO constrained. Daytime maximum OH concentration with HONO ($6.1 \times 10^6 \text{ cm}^{-3}$) was simulated to be 59% higher than the simulation without HONO ($3.9 \times 10^6 \text{ cm}^{-3}$), and the daily maximum concentration of O₃ with HONO (43.2 ppbv) was simulated to be 68.8% higher than the simulation without HONO (25.6 ppbv). These results are both within the range of prior studies (Elshorbany et al., 2012; Fu et al., 2019; Gil et al., 2021; Liu et al., 2021; Malkin et al., 2016; Xue et al., 2020; Yang et al., 2021a; Yun et al., 2017; Zhang et al., 2016), suggesting a strong HONO enhancement effect on atmospheric oxidation capacity. In addition, the impact of HONO on O₃ appeared two hours later than on OH, likely reflecting that HO₂ and RO₂, which are key proxy radicals in O₃ production were not significantly higher during early morning hours, despite higher HONO and OH.

540

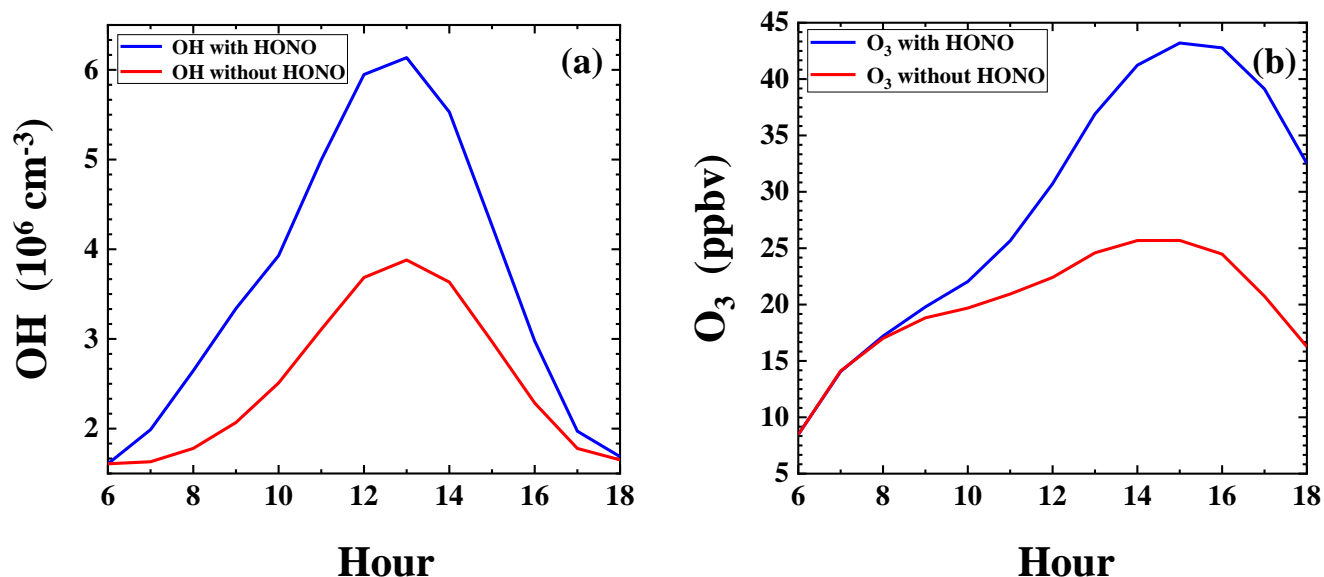


Figure 10. The diurnal variations of simulated O₃ and OH output with and without the HONO constrained in model.

4 Conclusions

Nitrous acid (HONO) was measured with a custom-built LOPAP instrument, along with meteorological parameters and other atmospheric constituents at an urban site in Guangzhou in Pearl River Delta from 27 September to 9 November 2018. The HONO concentrations varied from 0.02 to 4.43 ppbv with an average of 0.74 ± 0.70 ppbv. Compared to prior measurements in Guangzhou, a decreasing trend of HONO can be seen along with improved air quality in the city over the past decade. The emission ratios (HONO/NO_x) were derived from an analysis of 11 fresh plumes, varying from 0.1% to 1.5% with an average value of $0.9\% \pm 0.4\%$. Using this estimated emission ratio and an estimate of NO_x emission rate extracted from a grid cell around our site in a high-resolution (3 km × 3 km) NO_x emission inventory, we estimated a primary HONO emission rate of 0.30 ± 0.15 ppbv h⁻¹, which turned out far larger (almost by an order of magnitude) than what would be estimated with a city-level NO_x emission estimate, which does not adequately represent NO_x emission rate specifically for the observation site. Thus, for future analysis of HONO data to properly estimate direct emission of HONO, we suggest that high quality emission data be used to reduce uncertainty. This is especially crucial for a site that receives nearby traffic emissions like ours. HONO produced by the homogeneous reaction of OH + NO at night was 0.26 ± 0.08 ppbv h⁻¹, which can be seen as secondary results from primary emission. They were both much higher than the observed increase rate of HONO (0.02 ppbv h⁻¹) during the night. Nighttime soil emission rate was calculated to be 0.019 ± 0.001 ppbv h⁻¹, which is comparable to the observed increase rate of HONO during night, thus further demonstrating the importance of direct emissions. In order to balance the nighttime HONO budget and assuming dry deposition to be the principle loss process, a dry deposition rate of at least 1.8 cm s^{-1} is required. Correlation analysis shows that the heterogeneous reaction of NO₂

related to NH_3 and RH may contribute to the nighttime HONO formation. Daytime HONO budget analysis revealed that in order to sustain the observed HONO concentration around 450 pptv despite fast photolysis of HONO, an additional unknown source production rate (P_{Unknown}) of 0.65 ± 0.46 ppbv h^{-1} was needed, in addition to the primary emission P_{emis} at 0.12 ± 0.01 ppbv h^{-1} , and the homogenous reaction source $P_{\text{OH+NO}}$ at 0.79 ± 0.61 ppbv h^{-1} . It is worth noting that the homogenous HONO source by $\text{NO} + \text{OH}$ appeared to be a stronger source of HONO than the unknown source (P_{Unknown}), because of high levels of NO at our site. Correlation analysis between P_{Unknown} and proxies of different mechanisms showed that P_{Unknown} appeared to be photo-enhanced, and yet the mechanism remains unclear. Aerosols should not be as important as ground as a heterogenous reaction media, as very weak correlation between P_{Unknown} and $\text{PM}_{2.5}$. Moreover, no correlations were found between P_{Unknown} and nitrate/ HNO_3 , NH_3 , SO_2 . We assessed the role of HONO in the production of OH and O_3 by calculating OH production rate as well as by simulating the chemistry with a box model (MCMv3.3.1). The average net formation rate of OH attributed to HONO, O_3 and ozonolysis of alkenes was $3.7 \times 10^6 \text{ cm}^{-3} \text{ s}^{-1}$, $4.9 \times 10^6 \text{ cm}^{-3} \text{ s}^{-1}$ and $3 \times 10^5 \text{ cm}^{-3} \text{ s}^{-1}$, respectively. Box model simulations confirmed strong HONO enhancement effect on OH and O_3 by 59% and 68.8%, respectively.

575 **Data availability**

HONO data, other trace gases data and meteorological data are available upon request from the corresponding author.

Contribution

Yihang Yu: Validation, Formal analysis, Writing - Original Draft, Visualization. **Peng Cheng:** Conceptualization, Methodology, Writing - Review & Editing, Supervision, Project administration, Funding acquisition. **Huirong Li:** Validation, Formal analysis, Investigation, Data Curation. **Wenda Yang:** Software, Investigation, Data Curation. **Baobin Han:** Investigation. **Wei Song:** Resources. **Weiwei Hu:** Resources. **Xinming Wang:** Resources. **Bin Yuan:** Resources. **Min Shao:** Resources. **Zhijiong Huang:** Resources. **Zhen Li:** Resources. **Junyu Zheng:** Resources. **Haichao Wang:** Writing - Review & Editing. **Xiaofang Yu:** Investigation.

Competing interests

585 The authors declare that they have no conflict of interest.

Acknowledgments

This work was funded by the National Key Research and Development Program of China (grant nos. 2018YFC0213904, 2017YFC0210104), Science and Technology Plan Projects in Guangzhou (grant no. 201804010115), the Guangdong Natural Science Funds for Distinguished Young Scholar (grant no. 2018B030306037), the Guangdong Innovative and Entrepreneurial Research Team Program (grant no. 2016ZT06N263), and the Special Fund Project for Science and Technology Innovation Strategy of Guangdong Province (grant no. 2019B121205004).

References

- Acker, K., Febo, A., Trick, S., Perrino, C., Bruno, P., Wiesen, P., Möller, D., Wieprecht, W., Auel, R., Giusto, M., Geyer, A., Platt, U., and Allegrini, I.: Nitrous acid in the urban area of Rome, *Atmospheric Environment*, 40, 3123-3133, <https://doi.org/10.1016/j.atmosenv.2006.01.028>, 2006.
- Alicke, B., Platt, U., and Stutz, J.: Impact of nitrous acid photolysis on the total hydroxyl radical budget during the Limitation of Oxidant Production/Pianura Padana Produzione di Ozono study in Milan, *Journal of Geophysical Research: Atmospheres*, 107, 8196, <https://doi.org/10.1029/2000JD000075>, 2002.
- Alicke, B., Geyer, A., Hofzumahaus, A., Holland, F., Konrad, S., Pätz, H. W., Schäfer, J., Stutz, J., Volz-Thomas, A., and Platt, U.: OH formation by HONO photolysis during the BERLIOZ experiment, *Journal of Geophysical Research: Atmospheres*, 108, 8247, <https://doi.org/10.1029/2001JD000579>, 2003.
- Ammann, M., Kalberer, M., Jost, D. T., Tobler, L., Rössler, E., Piguet, D., Gägger, H. W., and Baltensperger, U.: Heterogeneous production of nitrous acid on soot in polluted air masses, *Nature*, 395, 157-160, <https://doi.org/10.1038/25965>, 1998.
- Ammar, R., Monge, M. E., George, C., and D'Anna, B.: Photoenhanced NO₂ Loss on Simulated Urban Grime, *ChemPhysChem*, 11, 3956-3961, <https://doi.org/10.1002/cphc.201000540>, 2010.
- An, J., Zhang, W., and Qu, Y.: Impacts of a strong cold front on concentrations of HONO, HCHO, O₃, and NO₂ in the heavy traffic urban area of Beijing, *Atmospheric Environment*, 43, 3454-3459, <https://doi.org/10.1016/j.atmosenv.2009.04.052>, 2009.
- Arens, F., Gutzwiller, L., Baltensperger, U., Gägger, H. W., and Ammann, M.: Heterogeneous Reaction of NO₂ on Diesel Soot Particles, *Environmental Science & Technology*, 35, 2191-2199, <https://doi.org/10.1021/es000207s>, 2001.
- Aubin, D. G., and Abbatt, J. P. D.: Interaction of NO₂ with Hydrocarbon Soot: Focus on HONO Yield, Surface Modification, and Mechanism, *The Journal of Physical Chemistry A*, 111, 6263-6273, <https://doi.org/10.1021/jp068884h>, 2007.
- Bejan, I., Abd-el-Aal, Y., Barnes, I., Benter, T., Bohn, B., Wiesen, P., and Kleffmann, J.: The photolysis of ortho-nitrophenols: a new gas phase source of HONO, *Phys Chem Chem Phys*, 8, 2028-2035, <http://dx.doi.org/10.1039/B516590C>, 2006.
- Brigante, M., Cazoir, D., D'Anna, B., George, C., and Donaldson, D. J.: Photoenhanced Uptake of NO₂ by Pyrene Solid Films, *The Journal of Physical Chemistry A*, 112, 9503-9508, <https://doi.org/10.1021/jp802324g>, 2008.
- Bröske, R., Kleffmann, J., and Wiesen, P.: Heterogeneous conversion of NO₂ on secondary organic aerosol surfaces: A possible source of nitrous acid (HONO) in the atmosphere?, *Atmos. Chem. Phys.*, 3, 469-474, <https://doi.org/10.5194/acp-3-469-2003>, 2003.
- Cazoir, D., Brigante, M., Ammar, R., D'Anna, B., and George, C.: Heterogeneous photochemistry of gaseous NO₂ on solid fluoranthene films: A source of gaseous nitrous acid (HONO) in the urban environment, *Journal of Photochemistry and Photobiology A: Chemistry*, 273, 23-28, <https://doi.org/10.1016/j.jphotochem.2013.07.016>, 2014.
- Chan, C. K., and Yao, X.: Air pollution in mega cities in China, *Atmospheric Environment*, 42, 1-42, <https://doi.org/10.1016/j.atmosenv.2007.09.003>, 2008.

- Cui, L., Li, R., Zhang, Y., Meng, Y., Fu, H., and Chen, J.: An observational study of nitrous acid (HONO) in Shanghai, China: The aerosol impact on HONO formation during the haze episodes, *Science of The Total Environment*, 630, 1057-1070, <https://doi.org/10.1016/j.scitotenv.2018.02.063>, 2018.
- Czader, B. H., Rappenglück, B., Percell, P., Byun, D. W., Ngan, F., and Kim, S.: Modeling nitrous acid and its impact on ozone and hydroxyl radical during the Texas Air Quality Study 2006, *Atmos. Chem. Phys.*, 12, 6939-6951, <https://doi.org/10.5194/acp-12-6939-2012>, 2012.
- Dillon, M. B., Lamanna, M. S., Schade, G. W., Goldstein, A. H., and Cohen, R. C.: Chemical evolution of the Sacramento urban plume: Transport and oxidation, *Journal of Geophysical Research: Atmospheres*, 107, ACH 3-1-ACH 3-15, <https://doi.org/10.1029/2001JD000969>, 2002.
- Donaldson, M. A., Berke, A. E., and Raff, J. D.: Uptake of Gas Phase Nitrous Acid onto Boundary Layer Soil Surfaces, *Environmental Science & Technology*, 48, 375-383, <https://doi.org/10.1021/es404156a>, 2014.
- Elshorbany, Y. F., Kurtenbach, R., Wiesen, P., Lissi, E., Rubio, M., Villena, G., Gramsch, E., Rickard, A. R., Pilling, M. J., and Kleffmann, J.: Oxidation capacity of the city air of Santiago, Chile, *Atmos. Chem. Phys.*, 9, 2257-2273, <https://doi.org/10.5194/acp-9-2257-2009>, 2009.
- Elshorbany, Y. F., Kleffmann, J., Kurtenbach, R., Lissi, E., Rubio, M., Villena, G., Gramsch, E., Rickard, A. R., Pilling, M. J., and Wiesen, P.: Seasonal dependence of the oxidation capacity of the city of Santiago de Chile, *Atmospheric Environment*, 44, 5383-5394, <https://doi.org/10.1016/j.atmosenv.2009.08.036>, 2010.
- Elshorbany, Y. F., Steil, B., Brühl, C., and Lelieveld, J.: Impact of HONO on global atmospheric chemistry calculated with an empirical parameterization in the EMAC model, *Atmos. Chem. Phys.*, 12, 9977-10000, <https://doi.org/10.5194/acp-12-9977-2012>, 2012.
- Fan, S., Wang, B., Tesche, M., Engelmann, R., Althausen, A., Liu, J., Zhu, W., Fan, Q., Li, M., Ta, N., Song, L., and Leong, K.: Meteorological conditions and structures of atmospheric boundary layer in October 2004 over Pearl River Delta area, *Atmospheric Environment*, 42, 6174-6186, <https://doi.org/10.1016/j.atmosenv.2008.01.067>, 2008.
- Febo, A., Perrino, C., and Allegrini, I.: Measurement of nitrous acid in milan, italy, by doas and diffusion denuders, *Atmospheric Environment*, 30, 3599-3609, [https://doi.org/10.1016/1352-2310\(96\)00069-6](https://doi.org/10.1016/1352-2310(96)00069-6), 1996.
- Feng, Y., Ning, M., Lei, Y., Sun, Y., Liu, W., and Wang, J.: Defending blue sky in China: Effectiveness of the “Air Pollution Prevention and Control Action Plan” on air quality improvements from 2013 to 2017, *Journal of Environmental Management*, 252, 109603, <https://doi.org/10.1016/j.jenvman.2019.109603>, 2019.
- Finlayson-Pitts, B. J., and Pitts, J. N.: CHAPTER 4 - Photochemistry of Important Atmospheric Species, in: *Chemistry of the Upper and Lower Atmosphere*, edited by: Finlayson-Pitts, B. J., and Pitts, J. N., Academic Press, San Diego, 86-129, 2000.
- Finlayson-Pitts, B. J., Wingen, L. M., Sumner, A. L., Syomin, D., and Ramazan, K. A.: The heterogeneous hydrolysis of NO₂ in laboratory systems and in outdoor and indoor atmospheres: An integrated mechanism, *Physical Chemistry Chemical Physics*, 5, 223-242, <https://doi.org/10.1039/B208564J>, 2003.
- Fu, X., Wang, T., Zhang, L., Li, Q., Wang, Z., Xia, M., Yun, H., Wang, W., Yu, C., Yue, D., Zhou, Y., Zheng, J., and Han, R.: The significant contribution of HONO to secondary pollutants during a severe winter pollution event in southern China, *Atmos. Chem. Phys.*, 19, 1-14, <https://doi.org/10.5194/acp-19-1-2019>, 2019.
- Ge, S., Wang, G., Zhang, S., Li, D., Xie, Y., Wu, C., Yuan, Q., Chen, J., and Zhang, H.: Abundant NH₃ in China Enhances Atmospheric HONO Production by Promoting the Heterogeneous Reaction of SO₂ with NO₂, *Environ Sci Technol*, 53, 14339-14347, <https://doi.org/10.1021/acs.est.9b04196>, 2019.
- Ge, Y., Shi, X., Ma, Y., Zhang, W., Ren, X., Zheng, J., and Zhang, Y.: Seasonality of nitrous acid near an industry zone in the Yangtze River Delta region of China: Formation mechanisms and contribution to the atmospheric oxidation capacity, *Atmospheric Environment*, 254, 118420, <https://doi.org/10.1016/j.atmosenv.2021.118420>, 2021.
- George, C., Strekowski, R. S., Kleffmann, J., Stemmler, K., and Ammann, M.: Photoenhanced uptake of gaseous NO₂ on solid organic compounds: a photochemical source of HONO?, *Faraday Discuss*, 130, 195-210; discussion 241-164, 519-124, <http://dx.doi.org/10.1039/B417888M>, 2005.
- Gil, J., Kim, J., Lee, M., Lee, G., Ahn, J., Lee, D. S., Jung, J., Cho, S., Whitehill, A., Szykman, J., and Lee, J.: Characteristics of HONO and its impact on O₃ formation in the Seoul Metropolitan Area during the Korea-US Air Quality study, *Atmospheric Environment*, 247, 118182, <https://doi.org/10.1016/j.atmosenv.2020.118182>, 2021.

- Hao, Q., Jiang, N., Zhang, R., Yang, L., and Li, S.: Characteristics, sources, and reactions of nitrous acid during winter at an urban site in the Central Plains Economic Region in China, *Atmos. Chem. Phys.*, 20, 7087-7102, <https://doi.org/10.5194/acp-20-7087-2020>, 2020.
- 680 Harrison, R. M., and Kitto, A.-M. N.: Evidence for a surface source of atmospheric nitrous acid, *Atmospheric Environment*, 28, 1089-1094, [https://doi.org/10.1016/1352-2310\(94\)90286-0](https://doi.org/10.1016/1352-2310(94)90286-0), 1994.
- Harrison, R. M., Peak, J. D., and Collins, G. M.: Tropospheric cycle of nitrous acid, *Journal of Geophysical Research: Atmospheres*, 101, 14429-14439, <https://doi.org/10.1029/96JD00341>, 1996.
- 685 Heard, D. E., Carpenter, L. J., Creasey, D. J., Hopkins, J. R., Lee, J. D., Lewis, A. C., Pilling, M. J., Seakins, P. W., Carslaw, N., and Emmerson, K. M.: High levels of the hydroxyl radical in the winter urban troposphere, *Geophysical Research Letters*, 31, <https://doi.org/10.1029/2004GL020544>, 2004.
- Heland, J., Kleffmann, J., Kurtenbach, R., and Wiesen, P.: A New Instrument To Measure Gaseous Nitrous Acid (HONO) in the Atmosphere, *Environmental Science & Technology*, 35, 3207-3212, <https://doi.org/10.1021/es000303t>, 2001.
- 690 Hendrick, F., Müller, J. F., Clémer, K., Wang, P., De Mazière, M., Fayt, C., Gielen, C., Hermans, C., Ma, J. Z., Pinardi, G., Stavrou, T., Vlemmix, T., and Van Roozendaal, M.: Four years of ground-based MAX-DOAS observations of HONO and NO₂ in the Beijing area, *Atmos. Chem. Phys.*, 14, 765-781, <https://doi.org/10.5194/acp-14-765-2014>, 2014.
- Hofzumahaus, A., Rohrer, F., Lu, K., Bohn, B., Brauers, T., Chang, C.-C., Fuchs, H., Holland, F., Kita, K., Kondo, Y., Li, X., Lou, S., Shao, M., Zeng, L., Wahner, A., and Zhang, Y.: Amplified Trace Gas Removal in the Troposphere, *Science*, 324, 1702-1704, <https://doi.org/10.1126/science.1164566>, 2009.
- 695 Hou, S., Tong, S., Ge, M., and An, J.: Comparison of atmospheric nitrous acid during severe haze and clean periods in Beijing, China, *Atmospheric Environment*, 124, 199-206, <https://doi.org/10.1016/j.atmosenv.2015.06.023>, 2016.
- Hu, M., Zhou, F., Shao, K., Zhang, Y., Tang, X., and Slanina, J.: Diurnal variations of aerosol chemical compositions and related gaseous pollutants in Beijing and Guangzhou, *J Environ Sci Health A Tox Hazard Subst Environ Eng*, 37, 479-488, <https://doi.org/10.1081/ESE-120003229>, 2002.
- 700 Huang, R. J., Yang, L., Cao, J., Wang, Q., Tie, X., Ho, K. F., Shen, Z., Zhang, R., Li, G., Zhu, C., Zhang, N., Dai, W., Zhou, J., Liu, S., Chen, Y., Chen, J., and O'Dowd, C. D.: Concentration and sources of atmospheric nitrous acid (HONO) at an urban site in Western China, *Science of The Total Environment*, 593-594, 165-172, <https://doi.org/10.1016/j.scitotenv.2017.02.166>, 2017.
- Huang, Z., Zhong, Z., Sha, Q., Xu, Y., Zhang, Z., Wu, L., Wang, Y., Zhang, L., Cui, X., Tang, M., Shi, B., Zheng, C., Li, 705 Z., Hu, M., Bi, L., Zheng, J., and Yan, M.: An updated model-ready emission inventory for Guangdong Province by incorporating big data and mapping onto multiple chemical mechanisms, *Science of The Total Environment*, 769, 144535, <https://doi.org/10.1016/j.scitotenv.2020.144535>, 2021.
- Indarto, A.: Heterogeneous reactions of HONO formation from NO₂ and HNO₃: a review, *Research on Chemical Intermediates*, 38, 1029-1041, <https://doi.org/10.1007/s1164-011-0439-z>, 2012.
- 710 Jenkin, M. E., Saunders, S. M., and Pilling, M. J.: The tropospheric degradation of volatile organic compounds: a protocol for mechanism development, *Atmospheric Environment*, 31, 81-104, [https://doi.org/10.1016/S1352-2310\(96\)00105-7](https://doi.org/10.1016/S1352-2310(96)00105-7), 1997.
- Jenkin, M. E., Saunders, S. M., Wagner, V., and Pilling, M. J.: Protocol for the development of the Master Chemical Mechanism, MCM v3 (Part B): tropospheric degradation of aromatic volatile organic compounds, *Atmos. Chem. Phys.*, 3, 181-193, <https://doi.org/10.5194/acp-3-181-2003>, 2003.
- 715 Jenkin, M. E., Young, J. C., and Rickard, A. R.: The MCM v3.3.1 degradation scheme for isoprene, *Atmos. Chem. Phys.*, 15, 11433-11459, <https://doi.org/10.5194/acp-15-11433-2015>, 2015.
- Jeon, W., Choi, Y., Souri, A. H., Roy, A., Diao, L., Pan, S., Lee, H. W., and Lee, S. H.: Identification of chemical fingerprints in long-range transport of burning induced upper tropospheric ozone from Colorado to the North Atlantic Ocean, 720 *Science of The Total Environment*, 613-614, 820-828, <https://doi.org/10.1016/j.scitotenv.2017.09.177>, 2018.
- Jiang, Y., Xue, L., Gu, R., Jia, M., Zhang, Y., Wen, L., Zheng, P., Chen, T., Li, H., Shan, Y., Zhao, Y., Guo, Z., Bi, Y., Liu, H., Ding, A., Zhang, Q., and Wang, W.: Sources of nitrous acid (HONO) in the upper boundary layer and lower free troposphere of the North China Plain: insights from the Mount Tai Observatory, *Atmos. Chem. Phys.*, 20, 12115-12131, <https://doi.org/10.5194/acp-20-12115-2020>, 2020.
- 725 Kaiser, E. W., and Wu, C. H.: A kinetic study of the gas phase formation and decomposition reactions of nitrous acid, *The Journal of Physical Chemistry*, 81, 1701-1706, <https://doi.org/10.1021/j100533a001>, 1977.

- Kalberer, M., Ammann, M., Arens, F., Gäggeler, H. W., and Baltensperger, U.: Heterogeneous formation of nitrous acid (HONO) on soot aerosol particles, *Journal of Geophysical Research: Atmospheres*, 104, 13825-13832, <https://doi.org/10.1029/1999JD900141>, 1999.
- 730 Kim, S., VandenBoer, T. C., Young, C. J., Riedel, T. P., Thornton, J. A., Swarthout, B., Sive, B., Lerner, B., Gilman, J. B., Warneke, C., Roberts, J. M., Guenther, A., Wagner, N. L., Dubé, W. P., Williams, E., and Brown, S. S.: The primary and recycling sources of OH during the NACHTT-2011 campaign: HONO as an important OH primary source in the wintertime, *Journal of Geophysical Research: Atmospheres*, 119, 6886-6896, <https://doi.org/10.1002/2013JD019784>, 2014.
- 735 Kirchstetter, T. W., Harley, R. A., and Littlejohn, D.: Measurement of Nitrous Acid in Motor Vehicle Exhaust, *Environmental Science & Technology*, 30, 2843-2849, <https://doi.org/10.1021/es960135y>, 1996.
- Kleffmann, J., Kurtenbach, R., Lörzer, J., Wiesen, P., Kalthoff, N., Vogel, B., and Vogel, H.: Measured and simulated vertical profiles of nitrous acid—Part I: Field measurements, *Atmospheric Environment*, 37, 2949-2955, [https://doi.org/10.1016/S1352-2310\(03\)00242-5](https://doi.org/10.1016/S1352-2310(03)00242-5), 2003.
- 740 Kleffmann, J., Gavriloiu, T., Hofzumahaus, A., Holland, F., Koppmann, R., Rupp, L., Schlosser, E., Siese, M., and Wahner, A.: Daytime formation of nitrous acid: A major source of OH radicals in a forest, *Geophysical Research Letters*, 32, <https://doi.org/10.1029/2005GL022524>, 2005.
- Kleffmann, J., Lörzer, J. C., Wiesen, P., Kern, C., Trick, S., Volkamer, R., Rodenas, M., and Wirtz, K.: Intercomparison of the DOAS and LOPAP techniques for the detection of nitrous acid (HONO), *Atmospheric Environment*, 40, 3640-3652, <https://doi.org/10.1016/j.atmosenv.2006.03.027>, 2006.
- 745 Kramer, L. J., Crilley, L. R., Adams, T. J., Ball, S. M., Pope, F. D., and Bloss, W. J.: Nitrous acid (HONO) emissions under real-world driving conditions from vehicles in a UK road tunnel, *Atmos. Chem. Phys.*, 20, 5231-5248, <https://doi.org/10.5194/acp-20-5231-2020>, 2020.
- Kurtenbach, R., Becker, K. H., Gomes, J. A. G., Kleffmann, J., Lörzer, J. C., Spittler, M., Wiesen, P., Ackermann, R., Geyer, A., and Platt, U.: Investigations of emissions and heterogeneous formation of HONO in a road traffic tunnel, *Atmospheric Environment*, 35, 3385-3394, [https://doi.org/10.1016/S1352-2310\(01\)00138-8](https://doi.org/10.1016/S1352-2310(01)00138-8), 2001.
- 750 Lammel, G., and Cape, J. N.: Nitrous acid and nitrite in the atmosphere, *Chemical Society Reviews*, 25, 361-369, <http://dx.doi.org/10.1039/CS9962500361>, 1996.
- Laufs, S., and Kleffmann, J.: Investigations on HONO formation from photolysis of adsorbed HNO₃ on quartz glass surfaces, *Phys Chem Chem Phys*, 18, 9616-9625, <https://doi.org/10.1039/C6CP00436A>, 2016.
- 755 Laufs, S., Cazaunau, M., Stella, P., Kurtenbach, R., Cellier, P., Mellouki, A., Loubet, B., and Kleffmann, J.: Diurnal fluxes of HONO above a crop rotation, *Atmos. Chem. Phys.*, 17, 6907-6923, <https://doi.org/10.5194/acp-17-6907-2017>, 2017.
- Lee, J. D., Whalley, L. K., Heard, D. E., Stone, D., Dunmore, R. E., Hamilton, J. F., Young, D. E., Allan, J. D., Laufs, S., and Kleffmann, J.: Detailed budget analysis of HONO in central London reveals a missing daytime source, *Atmos. Chem. Phys.*, 16, 2747-2764, <https://doi.org/10.5194/acp-16-2747-2016>, 2016.
- 760 Lelieveld, J., Gromov, S., Pozzer, A., and Taraborrelli, D.: Global tropospheric hydroxyl distribution, budget and reactivity, *Atmos. Chem. Phys.*, 16, 12477-12493, <https://doi.org/10.5194/acp-16-12477-2016>, 2016.
- Li, D., Xue, L., Wen, L., Wang, X., Chen, T., Mellouki, A., Chen, J., and Wang, W.: Characteristics and sources of nitrous acid in an urban atmosphere of northern China: Results from 1-yr continuous observations, *Atmospheric Environment*, 182, 296-306, <https://doi.org/10.1016/j.atmosenv.2018.03.033>, 2018a.
- 765 Li, G., Lei, W., Zavala, M., Volkamer, R., Dusanter, S., Stevens, P., and Molina, L. T.: Impacts of HONO sources on the photochemistry in Mexico City during the MCMA-2006/MILAGO Campaign, *Atmos. Chem. Phys.*, 10, 6551-6567, <https://doi.org/10.5194/acp-10-6551-2010>, 2010.
- Li, H., Cheng, P., Yu, Y., and Yang, W.: Nitrous acid (HONO) budget analysis at a rural site in the North China Plain during snowy days, in preparation.
- 770 Li, J., Lu, K., Lv, W., Li, J., Zhong, L., Ou, Y., Chen, D., Huang, X., and Zhang, Y.: Fast increasing of surface ozone concentrations in Pearl River Delta characterized by a regional air quality monitoring network during 2006–2011, *Journal of Environmental Sciences*, 26, 23-36, [https://doi.org/10.1016/S1001-0742\(13\)60377-0](https://doi.org/10.1016/S1001-0742(13)60377-0), 2014a.
- 775 Li, L., Duan, Z., Li, H., Zhu, C., Henkelman, G., Francisco, J. S., and Zeng, X. C.: Formation of HONO from the NH₃ promoted hydrolysis of NO₂ dimers in the atmosphere, *Proceedings of the National Academy of Sciences*, 115, 7236-7241, <https://doi.org/10.1073/pnas.1807719115>, 2018b.

- Li, X., Brauers, T., Häsel, R., Bohn, B., Fuchs, H., Hofzumahaus, A., Holland, F., Lou, S., Lu, K. D., Rohrer, F., Hu, M., Zeng, L. M., Zhang, Y. H., Garland, R. M., Su, H., Nowak, A., Wiedensohler, A., Takegawa, N., Shao, M., and Wahner, A.: Exploring the atmospheric chemistry of nitrous acid (HONO) at a rural site in Southern China, *Atmos. Chem. Phys.*, 12, 1497-1513, <https://doi.org/10.5194/acp-12-1497-2012>, 2012.
- Li, X., Rohrer, F., Hofzumahaus, A., Brauers, T., Häsel, R., Bohn, B., Broch, S., Fuchs, H., Gomm, S., Holland, F., Jäger, J., Kaiser, J., Keutsch, F. N., Lohse, I., Lu, K., Tillmann, R., Wegener, R., Wolfe, G. M., Mentel, T. F., Kiendler-Scharr, A., and Wahner, A.: Missing Gas-Phase Source of HONO Inferred from Zeppelin Measurements in the Troposphere, *Science*, 344, 292-296, <https://doi.org/10.1126/science.1248999>, 2014b.
- Li, Y., An, J., Min, M., Zhang, W., Wang, F., and Xie, P.: Impacts of HONO sources on the air quality in Beijing, Tianjin and Hebei Province of China, *Atmospheric Environment*, 45, 4735-4744, <https://doi.org/10.1016/j.atmosenv.2011.04.086>, 2011.
- Liao, B., Huang, J., Wang, C., Weng, J., Li, L., Cai, H., and D, W.: Comparative analysis on the boundary layer features of haze processes and cleaning process in Guangzhou, China *Environmental Science*, 38, 4432-4443, DOI:10.19674/j.cnki.issn1000-6923.2018.0496, 2018.
- Liao, W., Wu, L., Zhou, S., Wang, X., and Chen, D.: Impact of Synoptic Weather Types on Ground-Level Ozone Concentrations in Guangzhou, China, *Asia-Pacific Journal of Atmospheric Sciences*, <https://doi.org/10.1007/s13143-020-00186-2>, 2020.
- Lin, Y.-C., Cheng, M.-T., Ting, W.-Y., and Yeh, C.-R.: Characteristics of gaseous HNO₂, HNO₃, NH₃ and particulate ammonium nitrate in an urban city of Central Taiwan, *Atmospheric Environment*, 40, 4725-4733, <https://doi.org/10.1016/j.atmosenv.2006.04.037>, 2006.
- Liu, J., Deng, H., Li, S., Jiang, H., Mekic, M., Zhou, W., Wang, Y., Loisel, G., Wang, X., and Gligorovski, S.: Light-Enhanced Heterogeneous Conversion of NO₂ to HONO on Solid Films Consisting of Fluorene and Fluorene/Na₂SO₄: An Impact on Urban and Indoor Atmosphere, *Environ Sci Technol*, 54, 11079-11086, <https://doi.org/10.1021/acs.est.0c02627>, 2020a.
- Liu, J., Liu, Z., Ma, Z., Yang, S., Yao, D., Zhao, S., Hu, B., Tang, G., Sun, J., Cheng, M., Xu, Z., and Wang, Y.: Detailed budget analysis of HONO in Beijing, China: Implication on atmosphere oxidation capacity in polluted megacity, *Atmospheric Environment*, 244, 117957, <https://doi.org/10.1016/j.atmosenv.2020.117957>, 2021.
- Liu, Y.: Observations and parameterized modelling of ambient nitrous acid (HONO) in the megacity areas of the eastern China, Ph.D. thesis. College of Environmental Sciences and Engineering, Peking University, China, 2017.
- Liu, Y., Lu, K., Li, X., Dong, H., Tan, Z., Wang, H., Zou, Q., Wu, Y., Zeng, L., Hu, M., Min, K. E., Kecorius, S., Wiedensohler, A., and Zhang, Y.: A Comprehensive Model Test of the HONO Sources Constrained to Field Measurements at Rural North China Plain, *Environ Sci Technol*, <https://doi.org/10.1021/acs.est.8b06367>, 2019a.
- Liu, Y., Nie, W., Xu, Z., Wang, T., Wang, R., Li, Y., Wang, L., Chi, X., and Ding, A.: Semi-quantitative understanding of source contribution to nitrous acid (HONO) based on 1 year of continuous observation at the SORPES station in eastern China, *Atmos. Chem. Phys.*, 19, 13289-13308, <https://doi.org/10.5194/acp-19-13289-2019>, 2019b.
- Liu, Y., Ni, S., Jiang, T., Xing, S., Zhang, Y., Bao, X., Feng, Z., Fan, X., Zhang, L., and Feng, H.: Influence of Chinese New Year overlapping COVID-19 lockdown on HONO sources in Shijiazhuang, *Science of The Total Environment*, 745, 141025, <https://doi.org/10.1016/j.scitotenv.2020.141025>, 2020b.
- Liu, Y., Zhang, Y., Lian, C., Yan, C., Feng, Z., Zheng, F., Fan, X., Chen, Y., Wang, W., Chu, B., Wang, Y., Cai, J., Du, W., Daellenbach, K. R., Kangasluoma, J., Bianchi, F., Kujansuu, J., Petäjä, T., Wang, X., Hu, B., Wang, Y., Ge, M., He, H., and Kulmala, M.: The promotion effect of nitrous acid on aerosol formation in wintertime in Beijing: the possible contribution of traffic-related emissions, *Atmos. Chem. Phys.*, 20, 13023-13040, <https://doi.org/10.5194/acp-20-13023-2020>, 2020c.
- Lou, S., Holland, F., Rohrer, F., Lu, K., Bohn, B., Brauers, T., Chang, C. C., Fuchs, H., Häsel, R., Kita, K., Kondo, Y., Li, X., Shao, M., Zeng, L., Wahner, A., Zhang, Y., Wang, W., and Hofzumahaus, A.: Atmospheric OH reactivities in the Pearl River Delta – China in summer 2006: measurement and model results, *Atmos. Chem. Phys.*, 10, 11243-11260, <https://doi.org/10.5194/acp-10-11243-2010>, 2010.
- Lu, K. D., Rohrer, F., Holland, F., Fuchs, H., Bohn, B., Brauers, T., Chang, C. C., Häsel, R., Hu, M., Kita, K., Kondo, Y., Li, X., Lou, S. R., Nehr, S., Shao, M., Zeng, L. M., Wahner, A., Zhang, Y. H., and Hofzumahaus, A.: Observation and

- modelling of OH and HO₂ concentrations in the Pearl River Delta 2006: a missing OH source in a VOC rich atmosphere, *Atmos. Chem. Phys.*, 12, 1541-1569, <https://doi.org/10.5194/acp-12-1541-2012>, 2012.
- 830 Lu, K. D., Hofzumahaus, A., Holland, F., Bohn, B., Brauers, T., Fuchs, H., Hu, M., Häsel, R., Kita, K., Kondo, Y., Li, X., Lou, S. R., Oebel, A., Shao, M., Zeng, L. M., Wahner, A., Zhu, T., Zhang, Y. H., and Rohrer, F.: Missing OH source in a suburban environment near Beijing: observed and modelled OH and HO₂ concentrations in summer 2006, *Atmos. Chem. Phys.*, 13, 1057-1080, <https://doi.org/10.5194/acp-13-1057-2013>, 2013.
- Lu, K. D., Rohrer, F., Holland, F., Fuchs, H., Brauers, T., Oebel, A., Dlugi, R., Hu, M., Li, X., Lou, S. R., Shao, M., Zhu, T., Wahner, A., Zhang, Y. H., and Hofzumahaus, A.: Nighttime observation and chemistry of HO_x in the Pearl River Delta and Beijing in summer 2006, *Atmos. Chem. Phys.*, 14, 4979-4999, <https://doi.org/10.5194/acp-14-4979-2014>, 2014.
- 835 Lu, X., Hong, J., Zhang, L., Cooper, O. R., Schultz, M. G., Xu, X., Wang, T., Gao, M., Zhao, Y., and Zhang, Y.: Severe Surface Ozone Pollution in China: A Global Perspective, *Environmental Science & Technology Letters*, 5, 487-494, <https://doi.org/10.1021/acs.estlett.8b00366>, 2018.
- Maljanen, M., Yli-Pirilä, P., Hytönen, J., Joutsensaari, J., and Martikainen, P. J.: Acidic northern soils as sources of atmospheric nitrous acid (HONO), *Soil Biology and Biochemistry*, 67, 94-97, <https://doi.org/10.1016/j.soilbio.2013.08.013>, 2013.
- 840 Malkin, T. L., Heard, D. E., Hood, C., Stocker, J., Carruthers, D., MacKenzie, I. A., Doherty, R. M., Vieno, M., Lee, J., Kleffmann, J., Laufs, S., and Whalley, L. K.: Assessing chemistry schemes and constraints in air quality models used to predict ozone in London against the detailed Master Chemical Mechanism, *Faraday Discuss*, 189, 589-616, <https://doi.org/10.1039/C5FD00218D>, 2016.
- 845 Marion, A., Morin, J., Gandolfo, A., Ormeño, E., D'Anna, B., and Wortham, H.: Nitrous acid formation on Zea mays leaves by heterogeneous reaction of nitrogen dioxide in the laboratory, *Environmental Research*, 193, 110543, <https://doi.org/10.1016/j.envres.2020.110543>, 2021.
- Martinez, M., Harder, H., Kovacs, T. A., Simpas, J. B., Bassis, J., Leshner, R., Brune, W. H., Frost, G. J., Williams, E. J., Stroud, C. A., Jobson, B. T., Roberts, J. M., Hall, S. R., Shetter, R. E., Wert, B., Fried, A., Alicke, B., Stutz, J., Young, V. L., White, A. B., and Zamora, R. J.: OH and HO₂ concentrations, sources, and loss rates during the Southern Oxidants Study in Nashville, Tennessee, summer 1999, *Journal of Geophysical Research: Atmospheres*, 108, <https://doi.org/10.1029/2003JD003551>, 2003.
- 850 Mebel, A. M., Lin, M. C., and Melius, C. F.: Rate Constant of the HONO + HONO → H₂O + NO + NO₂ Reaction from ab Initio MO and TST Calculations, *The Journal of Physical Chemistry A*, 102, 1803-1807, <https://doi.org/10.1021/jp973449w>, 1998.
- Meng, F., Qin, M., Tang, K., Duan, J., Fang, W., Liang, S., Ye, K., Xie, P., Sun, Y., Xie, C., Ye, C., Fu, P., Liu, J., and Liu, W.: High-resolution vertical distribution and sources of HONO and NO₂ in the nocturnal boundary layer in urban Beijing, China, *Atmos. Chem. Phys.*, 20, 5071-5092, <https://doi.org/10.5194/acp-20-5071-2020>, 2020.
- 860 Meusel, H., Kuhn, U., Reiffs, A., Mallik, C., Harder, H., Martinez, M., Schuladen, J., Bohn, B., Parchatka, U., Crowley, J. N., Fischer, H., Tomsche, L., Novelli, A., Hoffmann, T., Janssen, R. H. H., Hartogensis, O., Pikridas, M., Vrekoussis, M., Bourtsoukidis, E., Weber, B., Lelieveld, J., Williams, J., Pöschl, U., Cheng, Y., and Su, H.: Daytime formation of nitrous acid at a coastal remote site in Cyprus indicating a common ground source of atmospheric HONO and NO, *Atmos. Chem. Phys.*, 16, 14475-14493, <https://doi.org/10.5194/acp-16-14475-2016>, 2016.
- 865 Meusel, H., Tamm, A., Kuhn, U., Wu, D., Leifke, A. L., Fiedler, S., Ruckteschler, N., Yordanova, P., Lang-Yona, N., Pöhlker, M., Lelieveld, J., Hoffmann, T., Pöschl, U., Su, H., Weber, B., and Cheng, Y.: Emission of nitrous acid from soil and biological soil crusts represents an important source of HONO in the remote atmosphere in Cyprus, *Atmos. Chem. Phys.*, 18, 799-813, <https://doi.org/10.5194/acp-18-799-2018>, 2018.
- Michoud, V., Kukui, A., Camredon, M., Colomb, A., Borbon, A., Miet, K., Aumont, B., Beekmann, M., Durand-Jolibois, R., Perrier, S., Zapf, P., Siour, G., Ait-Helal, W., Locoge, N., Sauvage, S., Afif, C., Gros, V., Furger, M., Ancellet, G., and Doussin, J. F.: Radical budget analysis in a suburban European site during the MEGAPOLI summer field campaign, *Atmos. Chem. Phys.*, 12, 11951-11974, <https://doi.org/10.5194/acp-12-11951-2012>, 2012.
- 870 Michoud, V., Colomb, A., Borbon, A., Miet, K., Beekmann, M., Camredon, M., Aumont, B., Perrier, S., Zapf, P., Siour, G., Ait-Helal, W., Afif, C., Kukui, A., Furger, M., Dupont, J. C., Haefelin, M., and Doussin, J. F.: Study of the unknown HONO daytime source at a European suburban site during the MEGAPOLI summer and winter field campaigns, *Atmos. Chem. Phys.*, 14, 2805-2822, <https://doi.org/10.5194/acp-14-2805-2014>, 2014.

- Ndour, M., D'Anna, B., George, C., Ka, O., Balkanski, Y., Kleffmann, J., Stemmler, K., and Ammann, M.: Photoenhanced uptake of NO₂ on mineral dust: Laboratory experiments and model simulations, *Geophysical Research Letters*, 35, <https://doi.org/10.1029/2007GL032006>, 2008.
- 880 Neuman, J. A., Trainer, M., Brown, S. S., Min, K.-E., Nowak, J. B., Parrish, D. D., Peischl, J., Pollack, I. B., Roberts, J. M., Ryerson, T. B., and Veres, P. R.: HONO emission and production determined from airborne measurements over the Southeast U.S, *Journal of Geophysical Research: Atmospheres*, 121, 9237-9250, <https://doi.org/10.1002/2016JD025197>, 2016.
- 885 Nie, W., Ding, A. J., Xie, Y. N., Xu, Z., Mao, H., Kerminen, V. M., Zheng, L. F., Qi, X. M., Huang, X., Yang, X. Q., Sun, J. N., Herrmann, E., Petäjä, T., Kulmala, M., and Fu, C. B.: Influence of biomass burning plumes on HONO chemistry in eastern China, *Atmos. Chem. Phys.*, 15, 1147-1159, <https://doi.org/10.5194/acp-15-1147-2015>, 2015.
- Oswald, R., Behrendt, T., Ermel, M., Wu, D., Su, H., Cheng, Y., Breuninger, C., Moravek, A., Mougín, E., Delon, C., Loubet, B., Pommerening-Röser, A., Sörgel, M., Pöschl, U., Hoffmann, T., Andreae, M. O., Meixner, F. X., and Trebs, I.: HONO Emissions from Soil Bacteria as a Major Source of Atmospheric Reactive Nitrogen, *Science*, 341, 1233-1235, <https://doi.org/10.1126/science.1242266>, 2013.
- 890 Pagsberg, P., Bjergbakke, E., Ratajczak, E., and Sillesen, A.: Kinetics of the gas phase reaction OH + NO(+M)→HONO(+M) and the determination of the UV absorption cross sections of HONO, *Chemical Physics Letters*, 272, 383-390, [https://doi.org/10.1016/S0009-2614\(97\)00576-9](https://doi.org/10.1016/S0009-2614(97)00576-9), 1997.
- Porada, P., Tamm, A., Raggio, J., Cheng, Y., Kleidon, A., Pöschl, U., and Weber, B.: Global NO and HONO emissions of biological soil crusts estimated by a process-based non-vascular vegetation model, *Biogeosciences*, 16, 2003-2031, <https://doi.org/10.5194/bg-16-2003-2019>, 2019.
- 895 Qin, M., Xie, P., Su, H., Gu, J., Peng, F., Li, S., Zeng, L., Liu, J., Liu, W., and Zhang, Y.: An observational study of the HONO–NO₂ coupling at an urban site in Guangzhou City, South China, *Atmospheric Environment*, 43, 5731-5742, <https://doi.org/10.1016/j.atmosenv.2009.08.017>, 2009.
- 900 Ren, X., Harder, H., Martinez, M., Leshner, R. L., Oligier, A., Simpás, J. B., Brune, W. H., Schwab, J. J., Demerjian, K. L., He, Y., Zhou, X., and Gao, H.: OH and HO₂ Chemistry in the urban atmosphere of New York City, *Atmospheric Environment*, 37, 3639-3651, [https://doi.org/10.1016/S1352-2310\(03\)00459-X](https://doi.org/10.1016/S1352-2310(03)00459-X), 2003.
- Ren, X., van Duin, D., Cazorla, M., Chen, S., Mao, J., Zhang, L., Brune, W. H., Flynn, J. H., Grossberg, N., Lefer, B. L., Rappenglück, B., Wong, K. W., Tsai, C., Stutz, J., Dibb, J. E., Thomas Jobson, B., Luke, W. T., and Kelley, P.: Atmospheric oxidation chemistry and ozone production: Results from SHARP 2009 in Houston, Texas, *Journal of Geophysical Research: Atmospheres*, 118, 5770-5780, <https://doi.org/10.1002/jgrd.50342>, 2013.
- 905 Rohrer, F., and Berresheim, H.: Strong correlation between levels of tropospheric hydroxyl radicals and solar ultraviolet radiation, *Nature*, 442, 184-187, <https://doi.org/10.1038/nature04924>, 2006.
- Saliba, N. A., Yang, H., and Finlayson-Pitts, B. J.: Reaction of Gaseous Nitric Oxide with Nitric Acid on Silica Surfaces in the Presence of Water at Room Temperature, *The Journal of Physical Chemistry A*, 105, 10339-10346, <https://doi.org/10.1021/jp012330r>, 2001.
- 910 Sarwar, G., Roselle, S. J., Mathur, R., Appel, W., Dennis, R. L., and Vogel, B.: A comparison of CMAQ HONO predictions with observations from the Northeast Oxidant and Particle Study, *Atmospheric Environment*, 42, 5760-5770, <https://doi.org/10.1016/j.atmosenv.2007.12.065>, 2008.
- Seinfeld, J. H., and Pandis, S. N.: *Atmospheric chemistry and physics: from air pollution to climate change*, John Wiley & Sons, 2016.
- 915 Shao, M., Ren, X., Wang, H., Zeng, L., Zhang, Y., and Tang, X.: Quantitative relationship between production and removal of OH and HO₂ radicals in urban atmosphere, *Chinese Science Bulletin*, 49, 2253-2258, <https://doi.org/10.1360/04wb0006>, 2004.
- Shi, X., Ge, Y., Zhang, Y., Ma, Y., and Zheng, J.: HONO observation and assessment of the effects of atmospheric oxidation capacity in Changzhou during the springtime of 2017, *Environmental Science*, v.41, 113-121, DOI: 10.13227/j.hjkx.201909032, 2020a.
- 920 Shi, X., Ge, Y., Zheng, J., Ma, Y., Ren, X., and Zhang, Y.: Budget of nitrous acid and its impacts on atmospheric oxidative capacity at an urban site in the central Yangtze River Delta region of China, *Atmospheric Environment*, 238, 117725, <https://doi.org/10.1016/j.atmosenv.2020.117725>, 2020b.

- 925 Slater, E. J., Whalley, L. K., Woodward-Massey, R., Ye, C., Lee, J. D., Squires, F., Hopkins, J. R., Dunmore, R. E., Shaw, M., Hamilton, J. F., Lewis, A. C., Crilley, L. R., Kramer, L., Bloss, W., Vu, T., Sun, Y., Xu, W., Yue, S., Ren, L., Acton, W. J. F., Hewitt, C. N., Wang, X., Fu, P., and Heard, D. E.: Elevated levels of OH observed in haze events during wintertime in central Beijing, *Atmos. Chem. Phys.*, 20, 14847-14871, <https://doi.org/10.5194/acp-20-14847-2020>, 2020.
- 930 Song, L., Deng, T., and Wu, D.: Study on planetary boundary layer height in a typical haze period and different weather types over Guangzhou, *Acta Scientiae Circumstantiae*, 39(5), 1381-1391, DOI: 10.13671/j.hjkxxb.2019.0080, 2019.
- Sörgel, M., Regelin, E., Bozem, H., Diesch, J. M., Drewnick, F., Fischer, H., Harder, H., Held, A., Hosaynali-Beygi, Z., Martinez, M., and Zetzsch, C.: Quantification of the unknown HONO daytime source and its relation to NO₂, *Atmos. Chem. Phys.*, 11, 10433-10447, <https://doi.org/10.5194/acp-11-10433-2011>, 2011a.
- 935 Sörgel, M., Trebs, I., Serafimovich, A., Moravek, A., Held, A., and Zetzsch, C.: Simultaneous HONO measurements in and above a forest canopy: influence of turbulent exchange on mixing ratio differences, *Atmos. Chem. Phys.*, 11, 841-855, <https://doi.org/10.5194/acp-11-841-2011>, 2011b.
- Sosedova, Y., Rouvière, A., Bartels-Rausch, T., and Ammann, M.: UVA/Vis-induced nitrous acid formation on polyphenolic films exposed to gaseous NO₂, *Photochemical & Photobiological Sciences*, 10, 1680-1690, <http://dx.doi.org/10.1039/C1PP05113J>, 2011.
- 940 Spindler, G., Brüggemann, E., and Herrmann, H.: Nitrous acid (HNO₂) concentration measurements and estimation of dry deposition over grassland in eastern Germany, *Proceedings of the EUROTRAC Symposium 1998*, Vol. 2, WITpress, Southampton, UK, 218-222, 1999.
- Stemmler, K., Ammann, M., Donders, C., Kleffmann, J., and George, C.: Photosensitized reduction of nitrogen dioxide on humic acid as a source of nitrous acid, *Nature*, 440, 195-198, <https://doi.org/10.1038/nature04603>, 2006.
- 945 Stutz, J., Kim, E. S., Platt, U., Bruno, P., Perrino, C., and Febo, A.: UV-visible absorption cross sections of nitrous acid, *Journal of Geophysical Research: Atmospheres*, 105, 14585-14592, <https://doi.org/10.1029/2000JD900003>, 2000.
- Stutz, J., Alicke, B., and Neftel, A.: Nitrous acid formation in the urban atmosphere: Gradient measurements of NO₂ and HONO over grass in Milan, Italy, *Journal of Geophysical Research: Atmospheres*, 107, 8192, <https://doi.org/10.1029/2001JD000390>, 2002.
- 950 Stutz, J., Alicke, B., Ackermann, R., Geyer, A., Wang, S., White, A. B., Williams, E. J., Spicer, C. W., and Fast, J. D.: Relative humidity dependence of HONO chemistry in urban areas, *Journal of Geophysical Research: Atmospheres*, 109, <https://doi.org/10.1029/2003JD004135>, 2004.
- Su, H.: HONO: a study to its sources and impacts from field measurements at the sub-urban areas of PRD region, Ph.D. thesis, College of Environmental Sciences and Engineering, Peking University, China, 2008.
- 955 Su, H., Cheng, Y. F., Cheng, P., Zhang, Y. H., Dong, S., Zeng, L. M., Wang, X., Slanina, J., Shao, M., and Wiedensohler, A.: Observation of nighttime nitrous acid (HONO) formation at a non-urban site during PRIDE-PRD2004 in China, *Atmospheric Environment*, 42, 6219-6232, <https://doi.org/10.1016/j.atmosenv.2008.04.006>, 2008a.
- Su, H., Cheng, Y. F., Shao, M., Gao, D. F., Yu, Z. Y., Zeng, L. M., Slanina, J., Zhang, Y. H., and Wiedensohler, A.: Nitrous acid (HONO) and its daytime sources at a rural site during the 2004 PRIDE-PRD experiment in China, *Journal of Geophysical Research*, 113, <https://doi.org/10.1029/2007JD009060>, 2008b.
- 960 Su, H., Cheng, Y., Oswald, R., Behrendt, T., Trebs, I., Meixner, F. X., Andreae, M. O., Cheng, P., Zhang, Y., and Pöschl, U.: Soil Nitrite as a Source of Atmospheric HONO and OH Radicals, *Science*, 333, 1616-1618, <https://doi.org/10.1126/science.1207687>, 2011.
- Tan, Z., Fuchs, H., Lu, K., Hofzumahaus, A., Bohn, B., Broch, S., Dong, H., Gomm, S., Häseler, R., He, L., Holland, F., 965 Li, X., Liu, Y., Lu, S., Rohrer, F., Shao, M., Wang, B., Wang, M., Wu, Y., Zeng, L., Zhang, Y., Wahner, A., and Zhang, Y.: Radical chemistry at a rural site (Wangdu) in the North China Plain: observation and model calculations of OH, HO₂ and RO₂ radicals, *Atmos. Chem. Phys.*, 17, 663-690, <https://doi.org/10.5194/acp-17-663-2017>, 2017.
- Tan, Z., Rohrer, F., Lu, K., Ma, X., Bohn, B., Broch, S., Dong, H., Fuchs, H., Gkatzelis, G. I., Hofzumahaus, A., Holland, F., Li, X., Liu, Y., Liu, Y., Novelli, A., Shao, M., Wang, H., Wu, Y., Zeng, L., Hu, M., Kiendler-Scharr, A., Wahner, 970 A., and Zhang, Y.: Wintertime photochemistry in Beijing: observations of ROx radical concentrations in the North China Plain during the BEST-ONE campaign, *Atmos. Chem. Phys.*, 18, 12391-12411, <https://doi.org/10.5194/acp-18-12391-2018>, 2018.
- Tan, Z., Lu, K., Hofzumahaus, A., Fuchs, H., Bohn, B., Holland, F., Liu, Y., Rohrer, F., Shao, M., Sun, K., Wu, Y., Zeng, L., Zhang, Y., Zou, Q., Kiendler-Scharr, A., Wahner, A., and Zhang, Y.: Experimental budgets of OH, HO₂, and RO₂ radicals

- 975 and implications for ozone formation in the Pearl River Delta in China 2014, *Atmos. Chem. Phys.*, 19, 7129-7150,
<https://doi.org/10.5194/acp-19-7129-2019>, 2019a.
- Tan, Z., Lu, K., Jiang, M., Su, R., Wang, H., Lou, S., Fu, Q., Zhai, C., Tan, Q., Yue, D., Chen, D., Wang, Z., Xie, S.,
Zeng, L., and Zhang, Y.: Daytime atmospheric oxidation capacity in four Chinese megacities during the photochemically
980 <https://doi.org/10.5194/acp-19-3493-2019>, 2019b.
- Tang, X. Y.: The characteristics of urban air pollution in China, in *Urbanization, energy, and air pollution in China: The
challenges ahead*, Proceedings of A Symposium, 47-54, DOI : 10.17226/11192, 2004.
- Tang, Y., An, J., Wang, F., Li, Y., Qu, Y., Chen, Y., and Lin, J.: Impacts of an unknown daytime HONO source on the
mixing ratio and budget of HONO, and hydroxyl, hydroperoxyl, and organic peroxy radicals, in the coastal regions of China,
985 *Atmos. Chem. Phys.*, 15, 9381-9398, <https://doi.org/10.5194/acp-15-9381-2015>, 2015.
- Tian, Z., Yang, W., Yu, X., Zhang, M., Zhang, H., Cheng, D., Cheng, P., and Wang, B.: HONO pollution characteristics
and nighttime sources during autumn in Guangzhou, China *Environmental Science*, 39 (05), 2000-2009, DOI: 10.13227/j.
hjkx.201709269, 2018.
- Tong, S., Hou, S., Zhang, Y., Chu, B., Liu, Y., He, H., Zhao, P., and Ge, M.: Comparisons of measured nitrous acid
990 (HONO) concentrations in a pollution period at urban and suburban Beijing, in autumn of 2014, *Science China Chemistry*,
58, 1393-1402, <https://doi.org/10.1007/s11426-015-5454-2>, 2015.
- Tong, S., Hou, S., Zhang, Y., Chu, B., Liu, Y., He, H., Zhao, P., and Ge, M.: Exploring the nitrous acid (HONO)
formation mechanism in winter Beijing: direct emissions and heterogeneous production in urban and suburban areas,
Faraday Discuss, 189, 213-230, <https://doi.org/10.1039/C5FD00163C>, 2016.
- 995 VandenBoer, T. C., Brown, S. S., Murphy, J. G., Keene, W. C., Young, C. J., Pszenny, A. A. P., Kim, S., Warneke, C., de
Gouw, J. A., Maben, J. R., Wagner, N. L., Riedel, T. P., Thornton, J. A., Wolfe, D. E., Dubé, W. P., Öztürk, F., Brock, C. A.,
Grossberg, N., Lefter, B., Lerner, B., Middlebrook, A. M., and Roberts, J. M.: Understanding the role of the ground surface in
HONO vertical structure: High resolution vertical profiles during NACHTT-11, *Journal of Geophysical Research:
Atmospheres*, 118, 10,155-110,171, <https://doi.org/10.1002/jgrd.50721>, 2013.
- 1000 VandenBoer, T. C., Young, C. J., Talukdar, R. K., Markovic, M. Z., Brown, S. S., Roberts, J. M., and Murphy, J. G.:
Nocturnal loss and daytime source of nitrous acid through reactive uptake and displacement, *Nature Geoscience*, 8, 55-60,
<https://doi.org/10.1038/ngeo2298>, 2015.
- Villena, G., Kleffmann, J., Kurtenbach, R., Wiesen, P., Lissi, E., Rubio, M. A., Croxatto, G., and Rappenglück, B.:
Vertical gradients of HONO, NOx and O₃ in Santiago de Chile, *Atmospheric Environment*, 45, 3867-3873,
1005 <https://doi.org/10.1016/j.atmosenv.2011.01.073>, 2011.
- Wang, G., Zhang, R., Gomez, M. E., Yang, L., Levy Zamora, M., Hu, M., Lin, Y., Peng, J., Guo, S., Meng, J., Li, J.,
Cheng, C., Hu, T., Ren, Y., Wang, Y., Gao, J., Cao, J., An, Z., Zhou, W., Li, G., Wang, J., Tian, P., Marrero-Ortiz, W., Secret,
J., Du, Z., Zheng, J., Shang, D., Zeng, L., Shao, M., Wang, W., Huang, Y., Wang, Y., Zhu, Y., Li, Y., Hu, J., Pan, B., Cai, L.,
Cheng, Y., Ji, Y., Zhang, F., Rosenfeld, D., Liss, P. S., Duce, R. A., Kolb, C. E., and Molina, M. J.: Persistent sulfate
1010 formation from London Fog to Chinese haze, *Proceedings of the National Academy of Sciences*, 113, 13630-13635,
<https://doi.org/10.1073/pnas.1616540113>, 2016.
- Wang, G., Ma, S., Niu, X., Chen, X., Liu, F., Li, X., Li, L., Shi, G., and Wu, Z.: Barrierless HONO and HOS(O)₂-NO₂
Formation via NH₃-Promoted Oxidation of SO₂ by NO₂, *The Journal of Physical Chemistry A*, 125, 2666-2672,
<https://doi.org/10.1021/acs.jpca.1c00539>, 2021.
- 1015 Wang, J., Zhang, X., Guo, J., Wang, Z., and Zhang, M.: Observation of nitrous acid (HONO) in Beijing, China:
Seasonal variation, nocturnal formation and daytime budget, *Science of The Total Environment*, 587-588, 350-359,
<https://doi.org/10.1016/j.scitotenv.2017.02.159>, 2017a.
- Wang, S., Zhou, R., Zhao, H., Wang, Z., Chen, L., and Zhou, B.: Long-term observation of atmospheric nitrous acid
(HONO) and its implication to local NO₂ levels in Shanghai, China, *Atmospheric Environment*, 77, 718-724,
1020 <https://doi.org/10.1016/j.atmosenv.2013.05.071>, 2013.
- Wang, T., Wei, X. L., Ding, A. J., Poon, C. N., Lam, K. S., Li, Y. S., Chan, L. Y., and Anson, M.: Increasing surface
ozone concentrations in the background atmosphere of Southern China, 1994-2007, *Atmos. Chem. Phys.*, 9, 6217-6227,
<https://doi.org/10.5194/acp-9-6217-2009>, 2009.

- 1025 Wang, T., Xue, L., Brimblecombe, P., Lam, Y. F., Li, L., and Zhang, L.: Ozone pollution in China: A review of concentrations, meteorological influences, chemical precursors, and effects, *Science of The Total Environment*, 575, 1582-1596, <https://doi.org/10.1016/j.scitotenv.2016.10.081>, 2017b.
- 1030 Weber, B., Wu, D., Tamm, A., Ruckteschler, N., Rodriguez-Caballero, E., Steinkamp, J., Meusel, H., Elbert, W., Behrendt, T., Sorgel, M., Cheng, Y., Crutzen, P. J., Su, H., and Poschl, U.: Biological soil crusts accelerate the nitrogen cycle through large NO and HONO emissions in drylands, *Proceedings of the National Academy of Sciences*, 112, 15384-15389, <https://doi.org/10.1073/pnas.1515818112>, 2015.
- 1035 Wen, L., Chen, T., Zheng, P., Wu, L., Wang, X., Mellouki, A., Xue, L., and Wang, W.: Nitrous acid in marine boundary layer over eastern Bohai Sea, China: Characteristics, sources, and implications, *Science of The Total Environment*, 670, 282-291, <https://doi.org/10.1016/j.scitotenv.2019.03.225>, 2019.
- 1040 Wojtal, P., Halla, J. D., and McLaren, R.: Pseudo steady states of HONO measured in the nocturnal marine boundary layer: a conceptual model for HONO formation on aqueous surfaces, *Atmos. Chem. Phys.*, 11, 3243-3261, <https://doi.org/10.5194/acp-11-3243-2011>, 2011.
- 1045 Wolfe, G. M., Marvin, M. R., Roberts, S. J., Travis, K. R., and Liao, J.: The Framework for 0-D Atmospheric Modeling (F0AM) v3.1, *Geosci. Model Dev.*, 9, 3309-3319, <https://doi.org/10.5194/gmd-9-3309-2016>, 2016.
- 1050 Wong, K. W., Oh, H. J., Lefer, B. L., Rappenglück, B., and Stutz, J.: Vertical profiles of nitrous acid in the nocturnal urban atmosphere of Houston, TX, *Atmos. Chem. Phys.*, 11, 3595-3609, <https://doi.org/10.5194/acp-11-3595-2011>, 2011.
- 1055 Wong, K. W., Tsai, C., Lefer, B., Haman, C., Grossberg, N., Brune, W. H., Ren, X., Luke, W., and Stutz, J.: Daytime HONO vertical gradients during SHARP 2009 in Houston, TX, *Atmos. Chem. Phys.*, 12, 635-652, <https://doi.org/10.5194/acp-12-635-2012>, 2012.
- 1060 Wu, C., Wu, D., and Yu, J. Z.: Quantifying black carbon light absorption enhancement with a novel statistical approach, *Atmos. Chem. Phys.*, 18, 289-309, <https://doi.org/10.5194/acp-18-289-2018>, 2018.
- 1065 Wu, D., Horn, M. A., Behrendt, T., Muller, S., Li, J., Cole, J. A., Xie, B., Ju, X., Li, G., Ermel, M., Oswald, R., Frohlich-Nowoisky, J., Hoor, P., Hu, C., Liu, M., Andreae, M. O., Poschl, U., Cheng, Y., Su, H., Trebs, I., Weber, B., and Sorgel, M.: Soil HONO emissions at high moisture content are driven by microbial nitrate reduction to nitrite: tackling the HONO puzzle, *ISME J*, 13, 1688-1699, <https://doi.org/10.1038/s41396-019-0379-y>, 2019.
- 1070 Wu, Y., Li, S., and Yu, S.: Monitoring urban expansion and its effects on land use and land cover changes in Guangzhou city, China, *Environmental Monitoring and Assessment*, 188, 54, <https://doi.org/10.1007/s10661-015-5069-2>, 2015.
- 1075 Xing, L., Wu, J., Elser, M., Tong, S., Liu, S., Li, X., Liu, L., Cao, J., Zhou, J., El-Haddad, I., Huang, R., Ge, M., Tie, X., Prévôt, A. S. H., and Li, G.: Wintertime secondary organic aerosol formation in Beijing–Tianjin–Hebei (BTH): contributions of HONO sources and heterogeneous reactions, *Atmos. Chem. Phys.*, 19, 2343-2359, <https://doi.org/10.5194/acp-19-2343-2019>, 2019.
- 1080 Xu, W., Kuang, Y., Zhao, C., Tao, J., Zhao, G., Bian, Y., Yang, W., Yu, Y., Shen, C., Liang, L., Zhang, G., Lin, W., and Xu, X.: NH₃-promoted hydrolysis of NO₂ induces explosive growth in HONO, *Atmos. Chem. Phys.*, 19, 10557-10570, <https://doi.org/10.5194/acp-19-10557-2019>, 2019.
- 1085 Xu, Z., Wang, T., Xue, L. K., Louie, P. K. K., Luk, C. W. Y., Gao, J., Wang, S. L., Chai, F. H., and Wang, W. X.: Evaluating the uncertainties of thermal catalytic conversion in measuring atmospheric nitrogen dioxide at four differently polluted sites in China, *Atmospheric Environment*, 76, 221-226, <https://doi.org/10.1016/j.atmosenv.2012.09.043>, 2013.
- 1090 Xu, Z., Wang, T., Wu, J., Xue, L., Chan, J., Zha, Q., Zhou, S., Louie, P. K. K., and Luk, C. W. Y.: Nitrous acid (HONO) in a polluted subtropical atmosphere: Seasonal variability, direct vehicle emissions and heterogeneous production at ground surface, *Atmospheric Environment*, 106, 100-109, <https://doi.org/10.1016/j.atmosenv.2015.01.061>, 2015.
- 1095 Xue, C., Zhang, C., Ye, C., Liu, P., Catoire, V., Krysztofiak, G., Chen, H., Ren, Y., Zhao, X., Wang, J., Zhang, F., Zhang, C., Zhang, J., An, J., Wang, T., Chen, J., Kleffmann, J., Mellouki, A., and Mu, Y.: HONO Budget and Its Role in Nitrate Formation in the Rural North China Plain, *Environ Sci Technol*, 54, 11048-11057, <https://doi.org/10.1021/acs.est.0c01832>, 2020.
- 1100 Xue, L., Gu, R., Wang, T., Wang, X., Saunders, S., Blake, D., Louie, P. K. K., Luk, C. W. Y., Simpson, I., Xu, Z., Wang, Z., Gao, Y., Lee, S., Mellouki, A., and Wang, W.: Oxidative capacity and radical chemistry in the polluted atmosphere of Hong Kong and Pearl River Delta region: analysis of a severe photochemical smog episode, *Atmos. Chem. Phys.*, 16, 9891-9903, <https://doi.org/10.5194/acp-16-9891-2016>, 2016.

- Xue, L. K., Wang, T., Gao, J., Ding, A. J., Zhou, X. H., Blake, D. R., Wang, X. F., Saunders, S. M., Fan, S. J., Zuo, H. C., Zhang, Q. Z., and Wang, W. X.: Ground-level ozone in four Chinese cities: precursors, regional transport and heterogeneous processes, *Atmos. Chem. Phys.*, 14, 13175-13188, <https://doi.org/10.5194/acp-14-13175-2014>, 2014.
- 1075 Yang, J., Shen, H., Guo, M.-Z., Zhao, M., Jiang, Y., Chen, T., Liu, Y., Li, H., Zhu, Y., Meng, H., Wang, W., and Xue, L.: Strong marine-derived nitrous acid (HONO) production observed in the coastal atmosphere of northern China, *Atmospheric Environment*, 244, 117948, <https://doi.org/10.1016/j.atmosenv.2020.117948>, 2021a.
- 1080 Yang, Q.: Observations and sources analysis of gaseous nitrous acid — A case study in Beijing and Pearl River Delta area, Ph.D. thesis, College of Environmental Sciences and Engineering, Peking University, China, 2014.
- Yang, Q., Su, H., Li, X., Cheng, Y., Lu, K., Cheng, P., Gu, J., Guo, S., Hu, M., Zeng, L., Zhu, T., and Zhang, Y.: Daytime HONO formation in the suburban area of the megacity Beijing, China, *Science China Chemistry*, 57, 1032-1042, <https://doi.org/10.1007/s11426-013-5044-0>, 2014.
- 1085 Yang, W., Cheng, P., Tian, Z., Zhang, H., Zhang, M., and Wang, B.: Study on HONO pollution characteristics and daytime unknown sources during summer and autumn in Guangzhou, China., *China Environmental Science*, 37 (006), 2029-2039, DOI: 10.3969/j.issn.1000-6923.2017.06.005, 2017a.
- 1090 Yang, W., Han, C., Zhang, T., Tang, N., Yang, H., and Xue, X.: Heterogeneous photochemical uptake of NO₂ on the soil surface as an important ground-level HONO source, *Environmental Pollution*, 271, 116289, <https://doi.org/10.1016/j.envpol.2020.116289>, 2021b.
- Yang, Y., Shao, M., KeBel, S., Li, Y., Lu, K., Lu, S., Williams, J., Zhang, Y., Zeng, L., Nölscher, A. C., Wu, Y., Wang, X., and Zheng, J.: How the OH reactivity affects the ozone production efficiency: case studies in Beijing and Heshan, China, *Atmos. Chem. Phys.*, 17, 7127-7142, <https://doi.org/10.5194/acp-17-7127-2017>, 2017b.
- 1095 Yang, Y., Li, X., Zu, K., Lian, C., Chen, S., Dong, H., Feng, M., Liu, H., Liu, J., Lu, K., Lu, S., Ma, X., Song, D., Wang, W., Yang, S., Yang, X., Yu, X., Zhu, Y., Zeng, L., Tan, Q., and Zhang, Y.: Elucidating the effect of HONO on O₃ pollution by a case study in southwest China, *Science of The Total Environment*, 756, 144127, <https://doi.org/10.1016/j.scitotenv.2020.144127>, 2021c.
- 1100 Ye, C., Zhou, X., Pu, D., Stutz, J., Festa, J., Spolaor, M., Cantrell, C., Mauldin, R. L., Weinheimer, A., and Haggerty, J.: ATMOSPHERIC SCIENCE. Comment on "Missing gas-phase source of HONO inferred from Zeppelin measurements in the troposphere", *Science*, 348, 1326, DOI: 10.1126/science.aaa1992, 2015.
- Ye, C., Gao, H., Zhang, N., and Zhou, X.: Photolysis of Nitric Acid and Nitrate on Natural and Artificial Surfaces, *Environ Sci Technol*, 50, 3530-3536, <https://doi.org/10.1021/acs.est.5b05032>, 2016.
- 1105 Ye, C., Zhang, N., Gao, H., and Zhou, X.: Photolysis of Particulate Nitrate as a Source of HONO and NO_x, *Environmental Science & Technology*, 51, 6849-6856, <https://doi.org/10.1021/acs.est.7b00387>, 2017.
- Yue, D. L., Hu, M., Wu, Z. J., Guo, S., Wen, M. T., Nowak, A., Wehner, B., Wiedensohler, A., Takegawa, N., Kondo, Y., Wang, X. S., Li, Y. P., Zeng, L. M., and Zhang, Y. H.: Variation of particle number size distributions and chemical compositions at the urban and downwind regional sites in the Pearl River Delta during summertime pollution episodes, *Atmos. Chem. Phys.*, 10, 9431-9439, <https://doi.org/10.5194/acp-10-9431-2010>, 2010.
- 1110 Yue, D. L., Zhong, L., Shen, J., Zhang, T., Zhou, Y., Zeng, L., and Dong, H.: Pollution properties of atmospheric HNO₂ and its effect on OH radical formation in the PRD region in autumn, *Environmental Science & Technology*, 162-166, DOI: 10.3969/j.issn.1003-6504.2016.02.030, 2016.
- Yun, H., Wang, Z., Zha, Q., Wang, W., Xue, L., Zhang, L., Li, Q., Cui, L., Lee, S., Poon, S. C. N., and Wang, T.: Nitrous acid in a street canyon environment: Sources and contributions to local oxidation capacity, *Atmospheric Environment*, 167, 223-234, <https://doi.org/10.1016/j.atmosenv.2017.08.018>, 2017.
- 1115 Yun, H.: Reactive nitrogen oxides (HONO, N₂O₅ and ClNO₂) in different atmospheric environment in China: concentrations formation and the impact on atmospheric oxidation capacity, Ph.D. thesis. Department of Civil and Environmental Engineering, The Hong Kong Polytechnic University, China, 2018.
- Zha, Q., Xue, L., Wang, T., Xu, Z., Yeung, C., Louie, P. K. K., and Luk, C. W. Y.: Large conversion rates of NO₂ to HNO₂ observed in air masses from the South China Sea: Evidence of strong production at sea surface?, *Geophysical Research Letters*, 41, 7710-7715, <https://doi.org/10.1002/2014GL061429>, 2014.
- 1120 Zhang, B., and Tao, F.-M.: Direct homogeneous nucleation of NO₂, H₂O, and NH₃ for the production of ammonium nitrate particles and HONO gas, *Chemical Physics Letters*, 489, 143-147, <https://doi.org/10.1016/j.cplett.2010.02.059>, 2010.

- Zhang, J., An, J., Qu, Y., Liu, X., and Chen, Y.: Impacts of potential HONO sources on the concentrations of oxidants and secondary organic aerosols in the Beijing-Tianjin-Hebei region of China, *Science of The Total Environment*, 647, 836-852, <https://doi.org/10.1016/j.scitotenv.2018.08.030>, 2019a.
- 1125 Zhang, L., Wang, T., Zhang, Q., Zheng, J., Xu, Z., and Lv, M.: Potential sources of nitrous acid (HONO) and their impacts on ozone: A WRF-Chem study in a polluted subtropical region, *Journal of Geophysical Research: Atmospheres*, 121, 3645-3662, <https://doi.org/10.1002/2015JD024468>, 2016.
- Zhang, N., Zhou, X., Shepson, P. B., Gao, H., Alaghmand, M., and Stirm, B.: Aircraft measurement of HONO vertical profiles over a forested region, *Geophysical Research Letters*, 36, <https://doi.org/10.1029/2009GL038999>, 2009.
- 1130 Zhang, W., Tong, S., Ge, M., An, J., Shi, Z., Hou, S., Xia, K., Qu, Y., Zhang, H., Chu, B., Sun, Y., and He, H.: Variations and sources of nitrous acid (HONO) during a severe pollution episode in Beijing in winter 2016, *Science of The Total Environment*, 648, 253-262, <https://doi.org/10.1016/j.scitotenv.2018.08.133>, 2019b.
- Zheng, J., Zhong, L., Wang, T., Louie, P. K. K., and Li, Z.: Ground-level ozone in the Pearl River Delta region: Analysis of data from a recently established regional air quality monitoring network, *Atmospheric Environment*, 44, 814-823, <https://doi.org/10.1016/j.atmosenv.2009.11.032>, 2010.
- 1135 Zheng, J., Shi, X., Ma, Y., Ren, X., Jabbour, H., Diao, Y., Wang, W., Ge, Y., Zhang, Y., and Zhu, W.: Contribution of nitrous acid to the atmospheric oxidation capacity in an industrial zone in the Yangtze River Delta region of China, *Atmos. Chem. Phys.*, 20, 5457-5475, <https://doi.org/10.5194/acp-20-5457-2020>, 2020.
- Zhong, L., Louie, P. K. K., Zheng, J., Yuan, Z., Yue, D., Ho, J. W. K., and Lau, A. K. H.: Science-policy interplay: Air quality management in the Pearl River Delta region and Hong Kong, *Atmospheric Environment*, 76, 3-10, <https://doi.org/10.1016/j.atmosenv.2013.03.012>, 2013.
- Zhou, X., Civerolo, K., Dai, H., Huang, G., Schwab, J., and Demerjian, K.: Summertime nitrous acid chemistry in the atmospheric boundary layer at a rural site in New York State, *Journal of Geophysical Research: Atmospheres*, 107, ACH 13-11-ACH 13-11, <https://doi.org/10.1029/2001JD001539>, 2002a.
- 1145 Zhou, X., He, Y., Huang, G., Thornberry, T. D., Carroll, M. A., and Bertman, S. B.: Photochemical production of nitrous acid on glass sample manifold surface, *Geophysical Research Letters*, 29, 26-21-26-24, <https://doi.org/10.1029/2002GL015080>, 2002b.
- Zhou, X., Gao, H., He, Y., Huang, G., Bertman, S. B., Civerolo, K., and Schwab, J.: Nitric acid photolysis on surfaces in low-NO_x environments: Significant atmospheric implications, *Geophysical Research Letters*, 30, <https://doi.org/10.1029/2003GL018620>, 2003.
- 1150 Zhou, X., Huang, G., Civerolo, K., Roychowdhury, U., and Demerjian, K. L.: Summertime observations of HONO, HCHO, and O₃ at the summit of Whiteface Mountain, New York, *Journal of Geophysical Research: Atmospheres*, 112, <https://doi.org/10.1029/2006JD007256>, 2007.
- Zhou, X., Zhang, N., TerAvest, M., Tang, D., Hou, J., Bertman, S., Alaghmand, M., Shepson, P. B., Carroll, M. A., Griffith, S., Dusanter, S., and Stevens, P. S.: Nitric acid photolysis on forest canopy surface as a source for tropospheric nitrous acid, *Nature Geoscience*, 4, 440-443, <https://doi.org/10.1038/ngeo1164>, 2011.
- 1155 Ziemba, L. D., Dibb, J. E., Griffin, R. J., Anderson, C. H., Whitlow, S. I., Lefer, B. L., Rappenglück, B., and Flynn, J.: Heterogeneous conversion of nitric acid to nitrous acid on the surface of primary organic aerosol in an urban atmosphere, *Atmospheric Environment*, 44, 4081-4089, <https://doi.org/10.1016/j.atmosenv.2008.12.024>, 2010.
- 1160